To the Graduate Council:

I am submitting herewith a thesis written by Chang Liu entitled “Mesophase Pitch-based Carbon Fiber and Its Composites: Preparation and Characterization.” I have examined the final electronic copy of this thesis for form and content and recommend that it be accepted in partial fulfillment of the requirements for the degree of Master of Science, with a major in Materials Science and Engineering.

Zhongren Yue, Major Professor

We have read this thesis
and recommend its acceptance:

Ahmad Vakili

William Hofmeister

Accepted for the Council:
Carolyn R. Hodges
Vice Provost and Dean of the Graduate School

(Original signatures are on file with official student records.)

Mesophase Pitch-based Carbon Fiber and Its Composites: Preparation and Characterization

A Thesis

Presented for the

Masters of Science

Degree

The University of Tennessee, Knoxville

Chang Liu

December 2010

DEDICATION

From the beginning of my UTSI experience I have received the kind help from uncountable number of people. The thesis that is presented here is based on the continuous effort of Dr.Yue, Dr.Vakili, and myself to research and to unlock the knowledge behind the University of Tennessee Space Institute's carbon fibers.

UTSI has given the opportunity to explore myself intellectually through the teachings from highly qualified world-class professors in mechanical and material science engineering programs. Without the challenges presented in class and in the lab I would not be where I am today.

ABSTRACT

The objective of this study is to investigate the relationship among process, structure, and property of the UTSI pitch-based carbon fibers and optimize carbon fiber's mechanical properties through the stabilization process. Various analysis techniques were employed throughout these investigations which include the Scanning Electron Microscope (SEM), optical microscope, Dia-stron system, MTS, and ImageJ.

Several fiber process techniques including fiber spinning, stabilization, and carbonization were explored to determine the effect of the thermal process on the fiber yield, fiber diameter, the sheath-core structure of stabilized fibers, the pac-man and hollow core structures of carbonized fibers, and the resulting mechanical properties of the carbon fibers. It was found that stabilization time and the temperature stepping had a great deal on influence on the resulting carbon fibers. Larger diameter fiber is easy to form sheath-core structure in the stabilization process. Pac-man structure was developed at 600°C during the carbonization. Both stabilization duration and the carbonization temperature control the resulting carbon fiber diameter and fiber structure defects such as the pac-man and hollow core defects. Multi-step stabilization can reduce the total stabilization duration and improve the mechanical properties of the resulting carbon fibers.

Fiber structure non-uniformities including fiber diameter distributions for a bundle fiber or along a single fiber, and pac-man angles were determined. Statistical analysis revealed the distribution of the carbon fiber cross-sectional areas and the result is compared against commercial available carbon fibers.

Carbon fiber sandwiched composites (CFSCs) were fabricated with UTSI carbon fiber and commercial PAN-based carbon fibers. Several configurations of sandwich structured composites were explored to test the flexural properties with varying sandwich thickness.

TABLE OF CONTENTS

LIST OF FIGURES

LIST OF TABLES

LIST OF ABBREVIATIONS

2S (2,3,4,5)	**Two(2) step stabilization in (2,3,4,5) hours**
4S2	**Four (4) step stabilization in two hours**
8S2	**Eight (8) step stabilization in two hours**
CF	**Carbon fiber**
CFSC	**Carbon fiber Sandwich Composite**
HB	**High bias stabilization**
HPCF	**High performance carbon fiber**
LB	**Low bias stabilization**
LPM	**Liters per minute**
LS	**Long stabilization**
NS	**Normal stabilization**
PAN	**Polyacrylonitrile**
SS	**Short stabilization**
SSC	**Sandwich Structured Composite**

Chapter 1: Introduction

1.1 Carbon Fibers and Their Composites:

1.1.1 Background of Carbon Fibers:

The origins of carbon fibers can be dated back to the days of Thomas Edison in 1880 [1]. It was around this time that Edison explored various ways to make filaments for the light bulb and unfortunately the carbon fibers he formed were insufficient for this particular task as they only had a lifetime of 40 hours. Much of history and the credit of inventions or new findings are up for debate and this can also be seen with the use of carbon fibers in light bulbs. In 1850, Joseph Wilson Swan started to use carbonized paper filaments to make the incandescent light bulb and he succeeded in 1878 to be the first person to invent a practical incandescent bulb that lasted 13.5 hours. The particular filament used by Swan's 1878 invention was derived from cotton [2].

After World War II the USAF undertook major efforts to become the best Air Force in the world. One of the initiatives was to develop state-of-the-art jet fighter planes. There are only two ways to improve the performance, in terms of acceleration and velocity, of any air or ground vehicle. The vehicle can either have a more powerful engine to generate more power or weight must be shed off the vehicle so that the power-to-weight ratio of the vehicle improves. Carbon fibers were explored by the USAF to be used in jet fighters as a way to reduce weight while still maintaining the chassis strength. Today majority of the fighters in the world utilize carbon fiber composites in their construction. USAF's F-22 airframe being 50% composite by weight [3], has over 350 carbon/epoxy parts and about a third (1/3) of the F-35 Joint Strike Fighter is made with carbon and glass fibers [4].

Utilization of carbon fibers is not only limited to Military applications as Civilian commercial industry plays a huge role in driving up the demand for carbon fibers in recent decades. Airbus is the second largest customer, after the Military, of commercial carbon fibers with its recent Super jumbo A380 and A350 made with great portions of carbon fibers. The third largest buyer is Boeing with the creation of its 787 Dreamliner

that contains about 50% carbon fiber [4]. The 787 is so fuel efficient that it can fly straight from England to Australia without stopping to refuel.

Top three buyers of carbon fiber utilize High Performance Carbon Fiber (HPCF). Carbon fibers are not limited to high performance applications and its use can also be found in Golf Clubs, Tennis Rackets, Laptop casing, and in many more regular commercial products. Widespread use of carbon fibers for vast applications is limited due to its high cost.

1.1.2 Manufacturing of Commercial Carbon Fibers:

The typical steps for manufacturing of commercial carbon fibers are shown in **Figure 1.1**. High cost of carbon fibers can mainly be attributed to the precursor [5]. Carbon fibers made from Polyacrylonitrile (PAN) precursor consists of 90% of the carbon fibers manufactured today.

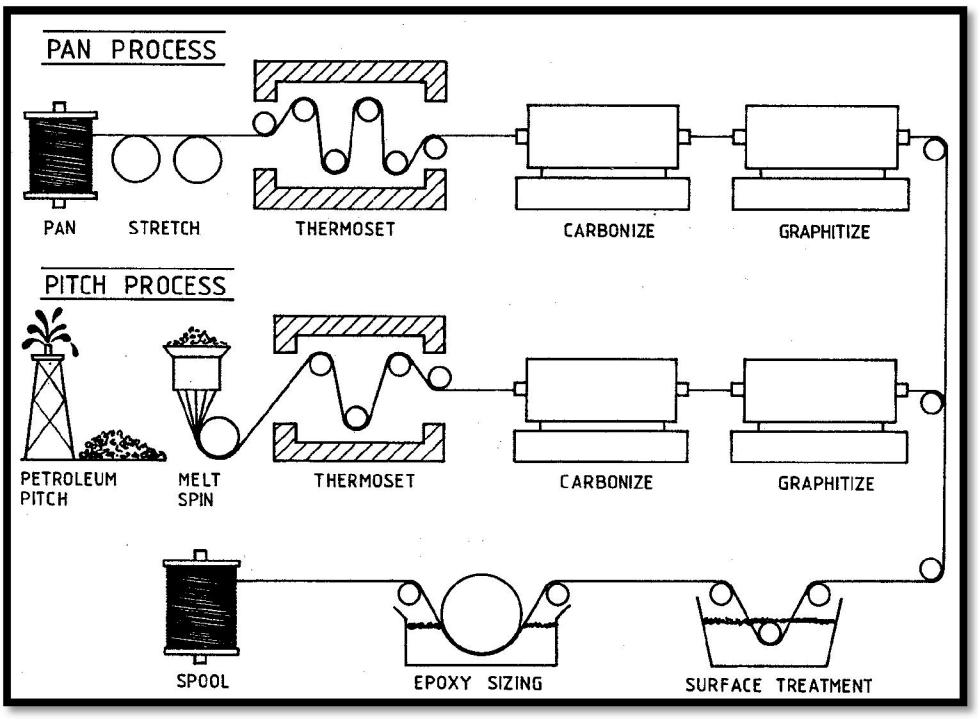

Figure 1.1 Manufacturing of PAN and Pitch carbon fibers [6]

PAN-based carbon fibers is expensive due to the high cost of PAN precursor and fiber spinning process, and the other manufacturing process involved in order to contain HPCF. Manufacturing of HPCF PAN fibers involves wet/dry melt spinning techniques that requires a costly wet chemical bath and a relatively long stabilization time. The search for a lower cost precursor for HPCF has led to the development of pitch-based carbon fibers.

Pitch-based carbon fibers can be manufactured in a similar process as PAN fibers. Pitch can be spun to fiber through melt spinning process which with costs relatively lower than wet/dry spinning. In melt spinning process the precursor is first heated until it exists in a liquid form and then it is pushed out from a spinneret. As the fiber comes out from the spinneret it is stretched and pulled to greatly reduce the fiber diameter to a desired value, meanwhile increase molecular orientation along the fiber axis and reduce the voids inside the fiber which result in higher strength and modulus.

After the fibers are formed it undergoes stabilization where the fibers are oxidized in air to introduce oxygen-containing groups while undergoing cross-linking. The stabilization process prevents the fiber from melting (fusion) again at higher temperatures. After that, Carbonization and graphitization follows stabilization and carries the process of aromatization and shedding non-carbon content to form a turbostratic graphite crystalline structure carbon fiber.

The primary advantage of pitch-based fibers is the high modulus as compared to PAN fibers. A high modulus fiber has many applications where the structure calls for high stiffness such as competitive Golf Clubs where ultrahigh modulus fibers provides better damping properties.

1.1.3 Preparation of UTSI Carbon Fibers:

Solvated mesophase pitch-based carbon fibers were first manufactured by Conoco-Philips using the melt blown technique. This research endeavor was passed onto UTSI via a donation by Conoco-Philips along with the spinning equipment and solvated mesophase pitch in 2004. The University of Tennessee Space Institute (UTSI) continues the development and application of such carbon fibers.

The UTSI spinning process is shown in **Figure 1.2**. Mesophase pitch precursor is heated until it melts in a closed system and then press through the spinneret. An air stream blows the melted precursor from the spinneret to form continuous long fibers that are collected as fiber tape (or non-woven mat).

The spun fibers (green fiber) are then thermally treated in a batch process. Green fiber are first dried to remove solvents and then oxidized in air to stabilize the green fiber. After stabilization the fiber undergoes carbonization at high temperature in an inert gas in a furnace.

The Preparation process of the UTSI carbon fiber can be simply described as follows [7-8]:

1. *Spinning* –Solvated mesophase pitch precursor is melted down into a liquid form and then sprayed out of spinning jets to form green or non-stabilized fibers. UTSI's spinning process is done by melt-blowing where the melted pitch is sprayed out of a spinneret jet and then drawn by blown hot air. During this process the fiber is drawn and stretched to maintain certain tension in the fiber so that the resulting fiber can have better molecular alignment along the fiber axis and a smaller diameter.
2. *Stabilization* – The green fiber, thermoplastic or non-stabilized fiber, requires dry oxidation to remove solvents from pitch and allow oxygen to diffuse into the fiber and strengthen the bonds through cross-linking so that it becomes thermally stabilized or thermoset. This process is done by subjecting the green fibers to temperatures from 150-400°C in air with varying temperature gradients and durations. If possible, tension could be applied and kept throughout stabilization to ensure better fiber axis alignment of molecules.
3. *Carbonization/graphitization* – This step follows stabilization or thermosetting where the stabilized fibers are heated between 1000-3000°C in an inert environment with either nitrogen (<1600^{o}C) or argon gas for a short duration. During carbonization all non-carbon elements are removed from the fiber, the fiber undergoes further cross-linking, and then resulting fiber becomes a carbon

fiber. Graphitization is simply carbonization at a high temperature such as 2000-3000°C.

4. *Surface treatment* – Carbon fibers have an inert surface which does not work well when trying to bond with polymeric resin matrices as the non-surface treated carbon fibers will experience slippage in the fiber/polymer composites. The fiber surface properties can be improved by surface treatments through various ways to provide a better adhesion to resins such as oxidation through air, carbon dioxide, ozone, nitric acid, or sodium hypochlorite.

The primary advantages of this technology are: 1) solvated mesophase pitch utilizes more fraction of raw pitch; 2) solvated pitch has lower soft point/melting point making pitch easier to spin; 3) high speed air blowing melting spinning is a high volume production fiber spinning process. As compared the conventional melt-spinning process, it greatly reduces the cost in the fiber spinning process; and 4) the spun pitch fiber can be stabilized with very short time. All these are expected to greatly reduce the cost of the resulting carbon fibers.

Figure 1.2 UTSI Pitch fiber spinning facility

However, there are problems with this novel fiber process that need to be addressed. The expression “There is no free lunch” describes the shortcomings of pitch-based carbon fibers as the melt-blowing process, with the micro vortices and turbulence, produces fibers that are kinky. One of the most important criteria for carbon fiber strength and modulus is the fiber alignment that is lacking in the UTSI produced pitch-based fibers.

1.1.4 Carbon Fiber Composites:

Carbon fibers primarily used in composites with a lightweight matrix. Carbon fiber composites are ideally suited to applications where strength, stiffness, lower weight, and outstanding fatigue characteristics are critical requirements. They also can be used in the occasion where high temperature durability, chemical inertness and high damping are important. The primary advantage of carbon fiber composites is in the high specific tensile strength and modulus as compared to steel and aluminum.

Many different carbon fiber composites are available in the markets and researches. These include polymer matrix composites, metal matrix composites, ceramic matrix composites, concrete matrix composites, and C/C composites [9]. The carbon fiber composites could be divided into fiber reinforced (short fiber and continuous fiber) and structural (laminar and sandwich) composites. Many technologies have been used to fabricate carbon fiber composites, including, contact molding, compression molding, vacuum molding, resin injection molding, filament winding, and pre-preg production processes [10].

A sandwich structured composite (**Figure 1.3**) is usually fabricated by attaching two thin but stiff skins to a lightweight but thick core. The core material is normally low strength material, but its higher thickness provides the sandwich composite with high bending stiffness with overall low density. In a composite sandwich structure, the core is responsible for separating and fixing the skins, resisting transverse shear, and providing other functionalities like absorbing impact energy, shielding radiation, and insulating heat transfer [11].

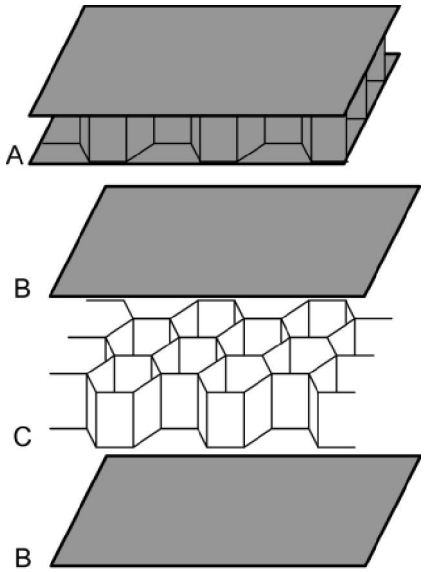

Figure 1.3 Sandwich structured composite with a honeycomb core*****

**http://en.wikipedia.org/wiki/Sandwich_structured_composite*

Sandwich structured composites have been widely used in satellites, aerospace structures, ship building, automobiles, rail cars, wind energy systems, bridge construction, and infrastructure due to their light weight and high strength to weight ratio. In the case of ground transportation, sandwich components have been successfully introduced to several applications such as roof panels in train and in bus structures, front cabins of high-speed locomotives, and interior panels. Minimizing the weight of a structure is becoming a common key design objective as it allows many options such as higher speed, longer range, larger payloads, less engine power and better operating economy.

1.2 Oxygen Diffusion in the Stabilization Process:

Diffusion of oxygen into pitch during the stabilization step is crucial for the prevention of fibers adhering to one another due to partial oxidation as well as producing desirable resulting mechanical properties of carbon fibers [12]. Control parameters in the diffusion process consist of stabilization time, heating rate, temperature, and pressure [13].

Stabilization requires the diffusion of oxygen into the green fiber, expulsion of trapped gases or possible solvents, and the cross-linking oxidative reaction to form a stabilized fiber. Oxidative reactions for pitch based green fibers start approximately beyond 180°C [14]. Rapid heating rates or short stabilization times can lead to the formation of sheath-core structures in both small diameter (10 µm) and large diameter (100 µm) fibers [12, 15]. Smaller fibers such as those of 10 µm in diameter are less affected by the oxidative reactions as compared to fibers of 100 µm in diameter [15]. The primary reason is that a thicker diameter requires more time for complete oxygen diffusion and the oxidative reactions occur from the outer layer to the core. Since the oxidative reaction lags behind the diffusion process the outer layers start to become fully oxidized while oxygen diffuses to the inner core. The ever more oxidized outer layers forms a sheath thereby restricting and preventing the diffusion of oxygen into the inner core forming the sheath-core structure.

Micro-thermal analysis done on 100 µm diameter mesophase pitch based fiber by Blanco, C., Lu, S., Appleyard, S.P., and Rand, B reveals that greater oxidation depth can be obtained with a greater stabilization time, 25 hours vs. 5 hours, for the same given stabilization temperature of 180°C [15]. Oxygen profiles obtained from the Micro-thermal analysis experiment shows that a more complete oxidation of the inner core and uniform oxidation of the entire fiber can be obtained at a lower stabilization temperature of 160°C vs. 200°C for the same stabilization time of 25 hours [15].

A similar study was conducted by Matsumoto, T., and Mochida, I. using tunneling Secondary Ion Mass Spectrometry (SIMS) and Elemental Analyzer on 10 µm diameter mesophase pitch obtained similar results. SIMS profile of the ratio of O_{16}/C_{12} reveals that 350°C is optimal stabilization temperature for the given heating rate of 0.5°C/min

[12]. This optimal temperature is different from the optimal uniform stabilization temperature of 160°C as found in the Micro-thermal analysis experiment [15]. The reason for this difference is that diffusion is not a major issue for a 10 µm fiber as compared to a 100 µm fiber where there exists less “layers” of semi-oxidized for fresh oxygen to fight through in order to penetrate to the fiber core. A quick stabilization forming a sheath core structure in a 100 µm diameter fiber with a 5 µm thick sheath will give the 10 µm fiber a complete oxidation because the sum of the penetration depth (sheath layer) from both sides is the total diameter for the 10 µm fiber. However, when the heating rate is changed from 0.5°C/min to 5.0°C/min higher temperature (300°C) stabilization proved to be less effective than lower temperature (230°C) stabilization for obtaining a uniform distribution of oxygen content within the fiber due to the formation of a sheath-core structure on the outer layers [12].

Successful attempts have been made to model diffusion of oxygen to pitch based fibers during stabilization. One study by Singer, L.S., and Mitchell, S. utilized electron paramagnetic resonance (EPR) to study the oxygen uptake by isotropic and mesophase pitch fibers from -50°C to 150°C and modeled the behavior with partial differential equations (PDEs) [14]. The dimensionless parameters of the partial differential equation (PDE) are diffusion rate, diffusion time, radius of fiber, and oxygen concentration with the assumption of isothermal conditions and constant barrier opposing oxygen diffusion or the non-formation of sheath-core structures throughout the stabilization process. The output of this PDE model was validated against previous findings literature and the results are consistent with other experimental findings [14]. Results from the model showed that a 10-fold increase in fiber diameter increases the fiber oxygen saturation time by nearly twice and a 100-fold increase in fiber diameter increases the fiber oxygen saturation time by nearly three times for the given fiber oxygen saturation levels of 50% and 90% [14]. This model can only be utilized for diffusion reactions of non-solvated isotropic and mesophase pitch for temperatures below 180-200°C because it assumes a constant barrier opposing oxygen diffusion. For temperatures above the 180°C the formation of sheath-core structures or a dynamic barrier opposing oxygen diffusion would make this a non-linear partial differential equation which involves a more rigorous mathematical treatment to find possible solutions. The addition of solvents in

mesophase pitch would also add to the difficulty of this type of PDE model as there are gases leaving the fiber during the oxygen diffusion into the fiber.

Another example of a model is in the study conducted by Liedtke, V., and Huttinger, K.J. on mesophase pitch fibers with X-ray photoelectron spectroscopy (XPS) and temperature-programmed desorption of surface functional groups (TPD). This experiment dealt with non-surface oxidized and surface-oxidized HT carbon fibers as well as mesogenic and mesophase pitch fibers. Control parameters were oxygen pressure (up to 2 MPa), temperature (160°C-200°C), and stabilization time (up to 36 hours). The diffusion model was based on Fick's 2nd law of diffusion where the fiber mass change during stabilization varied directly with the stabilization time for a given constant temperature [13]. Influence of oxygen pressure followed a power law where the fiber mass change during stabilization varied directly with the oxygen pressure raised to a pitch-specific exponential factor. Optimal fiber oxygen uptake was found to occur with 200°C and 1 MPa of oxygen pressure [13]. This study also circumvented the issue of sheath-core formation by purposefully maintaining a stabilization temperature no higher than 200°C to keep the stabilization process as diffusion controlled process rather than a reaction or oxidative controlled process. In a continuous industrial production process for low-cost carbon fibers it is very difficult and costly to perform stabilization around 1 MPa (~10 atm).

From the studies above it can be concluded that the fiber diameter dictates the optimal stabilization temperature and time. Larger diameter fibers are more prone to formation of sheath-core structures if the stabilization temperature goes well above 200°C before having significant oxygen saturation to the fiber core. A slower heating rate is ideal for obtaining a more uniformly stabilized fiber at the expense of having a much longer stabilization time. The diffusion process can be modeled in simplified conditions where the temperature is kept below 200°C threshold of sheath-core formation. The addition of pressure to stabilization allows for a more thorough oxidation of the fiber core but it is entirely impractical in a mass-production setting. The results in the literatures presented above on low temperature stabilization and slow heating rate along with inspirations from other literary sources play a crucial role in the pursuit of an optimal heating profile for UTSI's pitch-based carbon fibers.

1.3 Research Motivation and Objective:

The development of a domestic, low-cost carbon fiber composite industry is a strategic national priority that could have significant impact on the energy use of various sectors of the U.S. economy [16]. Being able to use lower cost precursors, produced in high volume, is a critical step toward lower cost carbon fiber composites for use in multiple industries.

Potential low-cost carbon fiber has been produced in our laboratory at the UTSI by using solvated mesophase pitch as precursor, a new-patented high-speed melt blown process to spin pitch fibers [17]. The prepared carbon fiber shows promising characteristic including small diameter (~7 μm), high electrical conductivity, and the appropriate mechanical properties. The carbon fiber was also fabricated to composites with different polymer resins. The composites show reasonable mechanical and physical properties.

However, since the UTSI carbon fiber process is different from the conventional carbon fiber process and utilizes special precursor and spinning method, the fundamental study on such novel carbon fibers is lacking. Few research papers have been published relating to the carbon fibers made from solvated mesophase pitch spun using melt blowing method. To further improve the properties of UTSI carbon fiber and its composites, and to reduce the process cost a fundamental study is critically needed.

It is well known that the structural uniformity of carbon fibers is very important in understanding the properties of fibers and the processing related issues to improve the fiber and fiber composite's quality and the performance. Therefore, the objective of this study is to:

- Investigate the effect of fiber spinning and thermal processes on fiber structure.
- Understand the relationship among stabilization conditions, structures, and properties.
- Examine and characterize the fiber diameter and structure uniformity.
- Test a new approach to the fabrication of carbon fiber composites.

Chapter 2: Materials and Methods

2.1 Materials:

2.1.1 Green Fibers:

Green fiber was used as starting material in this study. The green fibers were converted to carbon fibers through thermal treatments of stabilization and then subsequent carbonization. Green fibers were produced at the UTSI's spin Lab and spun from the ConocoPhillips solvated mesophase pitch through a melt-blown spinning process. The spun fiber (**Figure 2.1**) is continuous with low tensile strength. The fiber form looks like tape or non-woven mat which is very different from the conventional commercially available pitch- or PAN-based carbon fibers. Four types of green fibers were used in this study. They were spun with different air blowing rates named 40, 60, 80, and 100 Liters per minute (LPM).

2.1.2 Carbon Fibers:

UTSI pitch-based and commercial PAN-based carbon fibers were employed to fabricate carbon fiber sandwiched composites. UTSI carbon fiber was prepared in the Spin lab with a relatively larger volume. A typical carbon fiber form used for fabricating composites is shown in **Figure 2.2**.

The mechanical properties of the UTSI carbon fibers are listed in **Table 2.1** Variations occur in carbon fibers from different spinning speeds of 40, 60, 80, 100 LPM, spinnerets utilized, batch-to-batch differences of the same spinning process, and different stabilization processes.

Albany Engineered Composites' twill weave PAN-based carbon fiber fabric shown in **Figure 2.3** was used as skin materials in this study for the construction of carbon fiber sandwiched composites.

Figure 2.1 UTSI green fiber

Table 2.1 The typical UTSI carbon fiber used for the fabrication of composites

Carbonization Temperature (°C)	Fiber diameter (μm)	Tensile Strength (MPa)	Tensile Modulus (GPa)
1050	10-20	500-900	~20

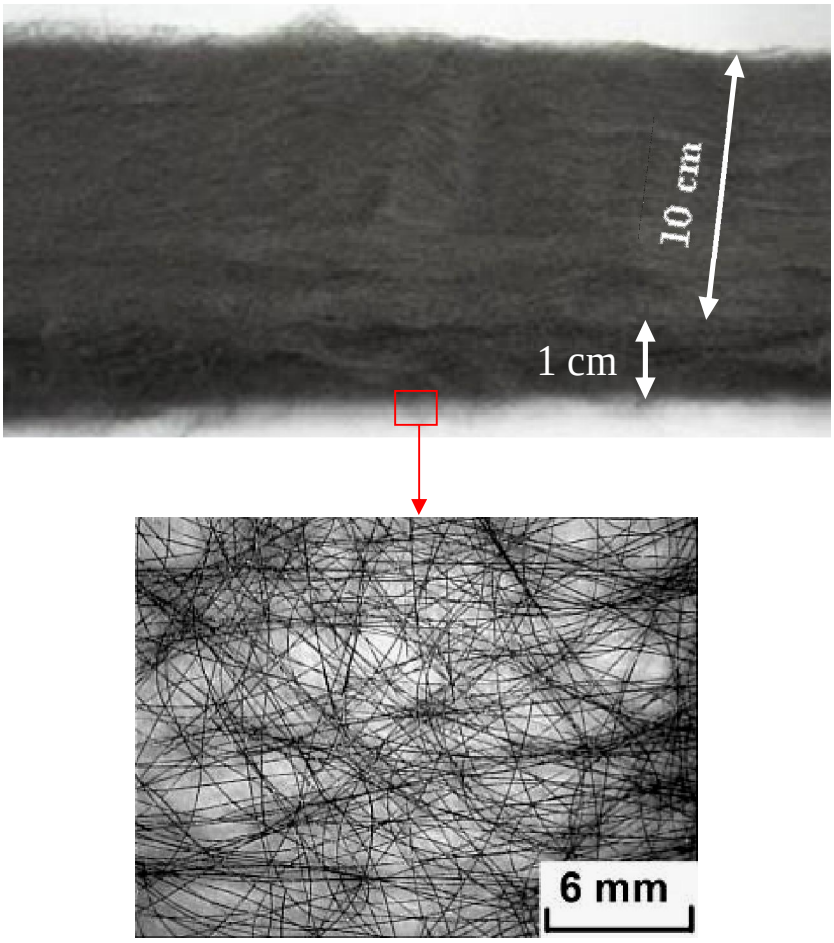

Figure 2.2 Typical UTSI carbon fiber form

Figure 2.3 Commercial PAN-based carbon fabric

2.1.3 Resins:

West System Epoxy 105 and Hardener 206 were used throughout the research process in making embedded samples for Optical microscope analysis as well as fabrication of carbon fiber composites.

2.2 Thermal Process:

2.2.1 Stabilization:

Various stabilization methods were employed to determine if stabilization had any impact on the micro-structure and tensile strength and modulus of the resulting carbon fiber. **Table 2.2** represents the various profiles explored with stabilization and carbonization parameters. For instance the initial stabilization method, normal stabilization (NS), consists of heating the tube furnace (**Figure 2.1**) to 350°C and holding the green fiber at that temperature for 60 minutes. Compressed air was used for the stabilization process for all stabilization methods explored.

Figure 2.4 Furnace for stabilization and carbonization

Table 2.2 Parameters for stabilization and carbonization

Sample	Temperature Profile	Stabilization		Carbon-ization Temp. (°C)
		Final Temp. (°C)	Holding Time (min)	
NS	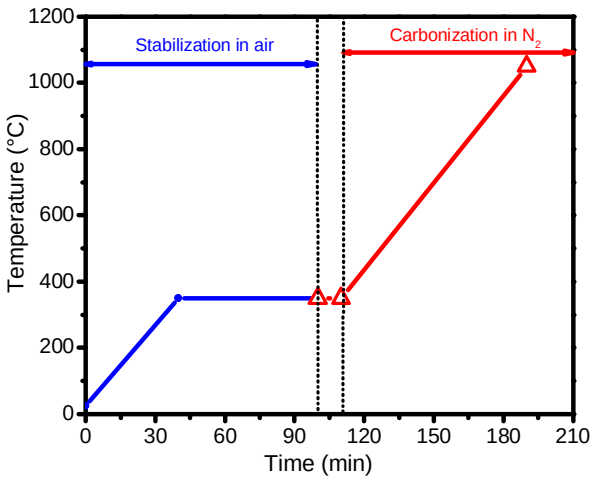	350	60	1050
4S2	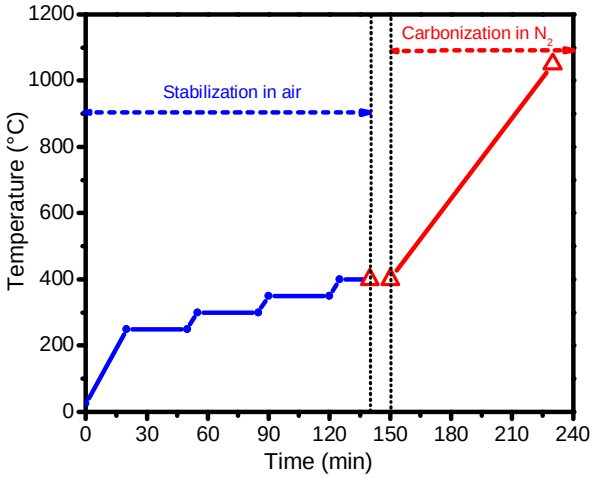	250 300 350 400	30 30 30 15	1050

Table 2.2 (continued)

LS	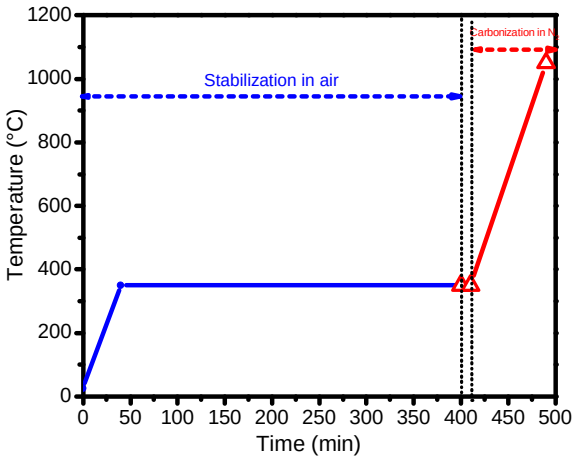	350	360	1050
2S2 2S3 2S4 2S5	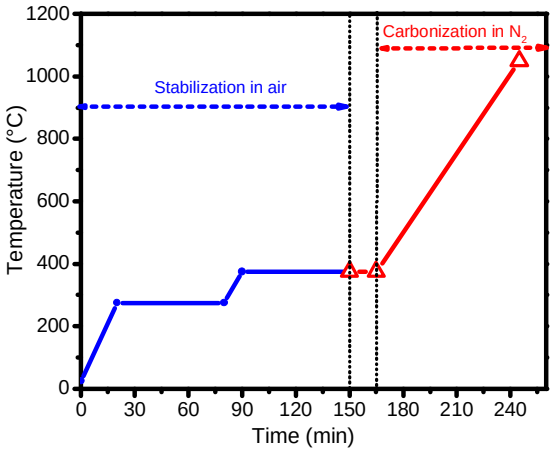	275 375	60,60 90,90 120,120 150,150	1050
8S2	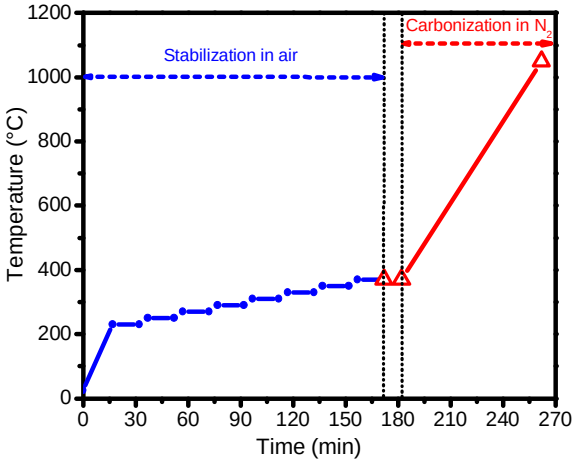	230 250 270 290 310 330 350 370	15 15 15 15 15 15 15 15	1050

Table 2.2 (continued)

LB	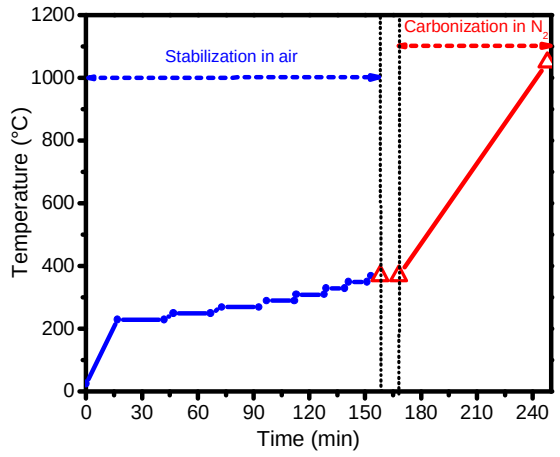	230 250 270 290 310 330 350 370	25 20 20 15 15 10 10 5	1050
HB	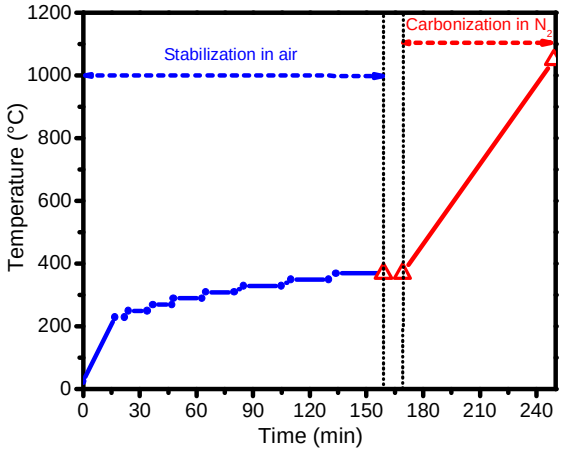	230 250 270 290 310 330 350 370	5 10 10 15 15 20 20 25	1050
SS	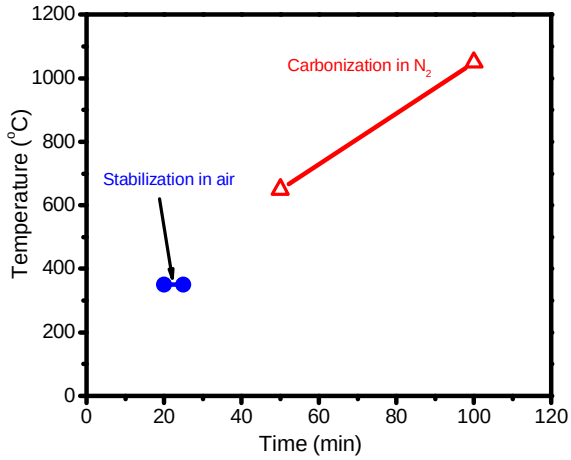	350	5	Fast carbon-ization at 600°C and then heat to 1050°C

2.2.2 Carbonization:

Carbonization follows stabilization which is done in an inert environment with Nitrogen (N_2). Stabilized fibers are placed in the Tube furnace (**Figure 2.4**) and then furnace is flushed out with N_2 to get rid of oxygen and trace amounts of other gasses that might react with the stabilized fiber during high temperatures. After the flushing process the furnace is set to 1050°C. Once the furnace reaches 1050°C it is held at that temperature for Five minutes then the furnace is turned off and left for cool down with a steady flow of N_2. The carbon fibers can be removed after the furnace cools down to about +50°C of room temperature. All temperature profiles used the same carbonization method as shown in **Table 2.2** with the exception of the last sample Short Stabilization (SS) in this table.

2.3 Fabrication of Carbon Fiber Sandwiched Composites:

2.3.1 Vacuum Bagging Resin Infusion:

Vacuum bagging resin infusion technique was used to fabricate carbon fiber sandwiched composites (CFSCs) and is shown in **Figure 2.5**. The vacuum helps the air bubbles to escape from the composite before curing and uniformly diffuse the epoxy resin solution throughout the entire composite. Addition of pressure from a hot press helps to compress the composite to improve fiber density of the composite.

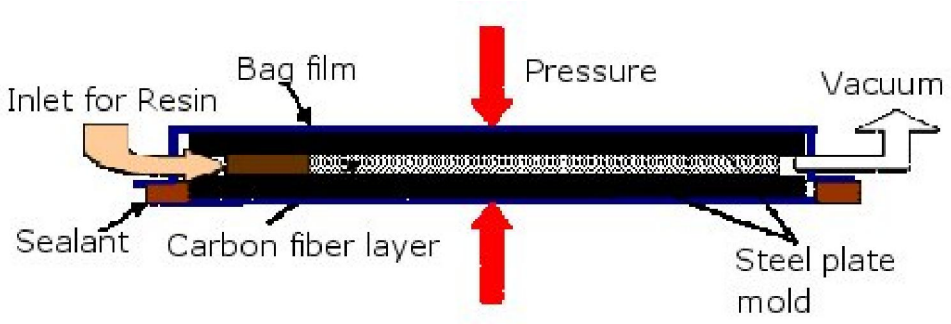

Figure 2.5 Vacuum bagging resin infusion method for making CFSCs

To make the composite with vacuum bagging resin infusion technique a few layers of carbon fiber sheets are placed between two steel plates covered with a release film as shown in **Figure 2.6** (A). The stack of carbon fibers with the steel plates are then placed between two vacuum bagging films, two tubes are fitted to the setup which serve as the inlet and outlet for the epoxy resin solution, and then the entire setup is sealed with vacuum sealant as shown in **Figure 2.6** (B). Hot plates help to lower the viscosity of the epoxy resin infusion to increase the diffusion rate (**Figure 2.7**). Adding pressure increases the fiber volume fraction of the carbon fiber composite by compacting the fiber layers and squeezing out the excess epoxy resin. After the epoxy resin solution is fully diffused, the fiber composite is cured slowly under pressure at elevated temperature from the press.

2.3.2 Sandwich Fabrication:

Carbon fiber sandwiched composites (CFSCs) were fabricated, in this study, using UTSI pitch-based carbon fiber composite as core materials and commercial PAN-based carbon fiber as skin materials. The UTSI CFSC panels prepared are shown in **Figure 2.8**

Fabrication procedure for the CFSCs is identical to that of vacuum bagging resin infusion. CFSC simply requires the addition of the outer skin of PAN fabric (**Figure 2.9**) to top and bottom the UTSI pitch carbon fiber stack before sandwiching the CFSC with the two steel plates and vacuum bagging resulting in a CFSC cross-section as shown in **Figure 2.9**.

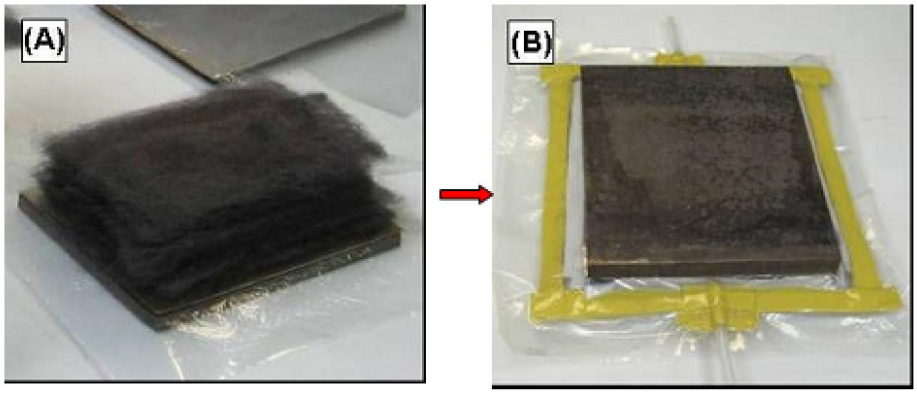

Figure 2.6 Vacuum bagging resin infusion procedure

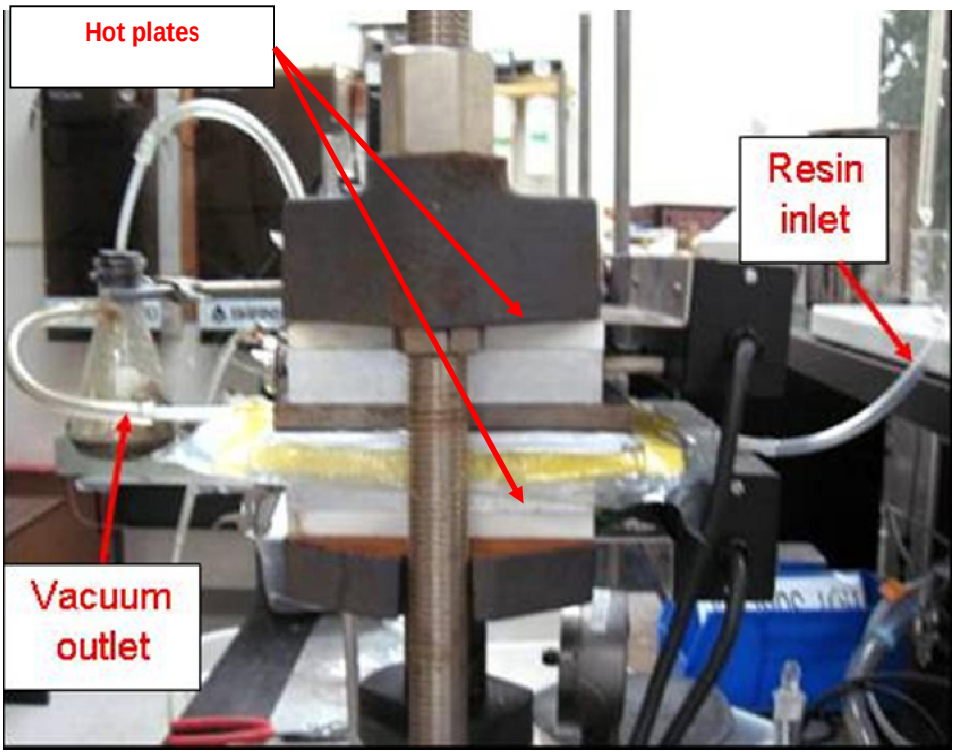

Figure 2.7 Vacuum bagging resin infusion with hot plate press

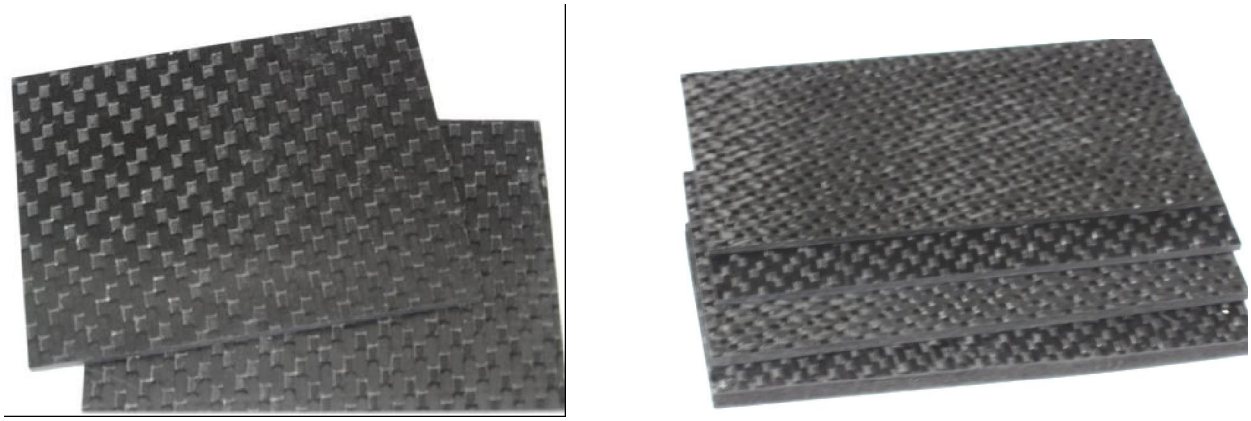

Figure 2.8 UTSI carbon fiber sandwiched composite panels

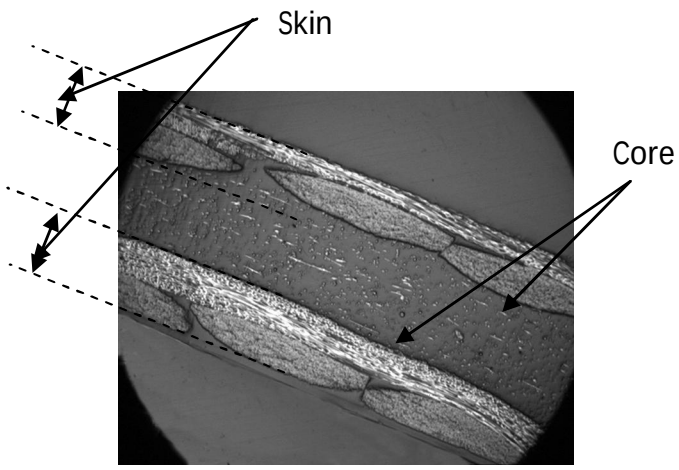

Figure 2.9 Cross-section of UTSI CFSC showing core (from UTSI pitch-based carbon fiber) and two skins (from PAN-based carbon fiber)

2.4 Measurement and Characterization:

2.4.1 Single-fiber Testing:

Individual fibers are picked from each method to ascertain their respective tensile strength and modulus. Fibers are mounted on plastic tabs by Jeweler's wax and placed on a tray. The tray holds 15 samples therefore 15 single fibers are chosen from each method for analysis. First the fiber is placed between the slots of the two tabs and then wax is applied to the square cup to secure to fiber to the tab. After all 15 fibers have been secured on the tabs an additional reheat sequence is done to assure a better bond between the wax and fiber. The rapid cooling rate on the droplet of wax does not allow for a very good bond to the surface of the fiber. If the tray of 15 fibers undergoes tensile testing without the reheat cycle the plot of the stress-strain curve will display abrupt spikes which usually results from fiber slippage in the wax. Applying the reheat cycle allows trapped air bubbles to escape, the wax to melt and bond firmly to the square cup, and most importantly allows the wax to melt and have a better adhesion to the surface of the fiber.

Fiber diameter and tensile properties were measured using a Dia-stron® system (**Figure 2.10**) which is comprised of the FDAS 765 laser scan micrometer, LEX 810 tensile tester (**Figure 2.10**), and controlled by the UV-Win software.

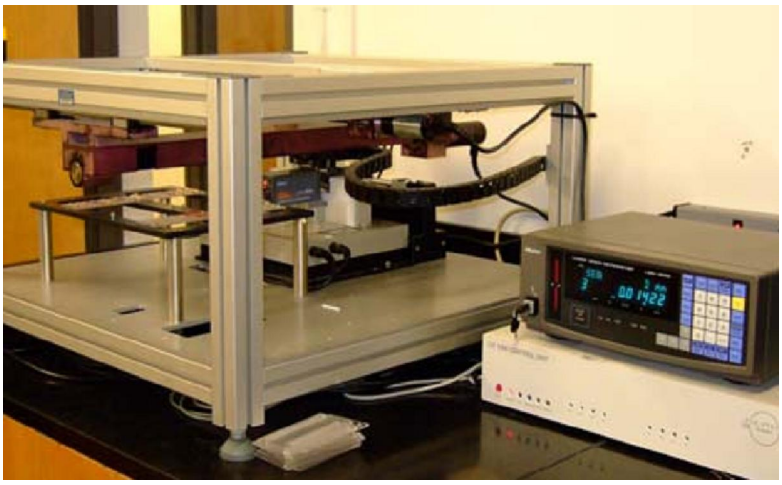

Figure 2.10 Dia-stron® system

The 15 samples are transferred first to the FDAS 765 laser scan micrometer to measure diameter of the fiber samples. This is measured by the Mitutoyo LSM 500 laser micrometer where the diameter is measured to be the difference between the emitted and the received laser beam. Measurements are taken at every 20° rotation and a full rotation of 180° is done for each segment or slice of the sample. The gauge length is 10 mm and there are 10 slices observed for each sample.

After measuring the diameter with the FDAS 765 laser scan micrometer the sample is moved to the LEX 810 tensile tester bench to measure the tensile strength. The LEX 810 tensile tester is comprised of a DC motor for drawing the fiber and a Sensotec semi-conductor strain gage load cell which measures the load on the sample. The pull rate for tensile testing is 0.01 mm/s, the gauge force is 0.2 gram force (gmf), the maximum force is 250 gmf, and the break threshold is set at three. By default UV-Win graphs Stress-strain curve with the Y-axis as gram force (gmf) and the X-axis as microns. Calculated results of tensile strength and modulus in Pascals are reported based on the minimum cross-sectional area which is the most likely break-point for the sample. The Y-axis units can be changed to Mega Pascals (MPa) from Gram force in which case the MPa is calculated based on the minimum cross-sectional area.

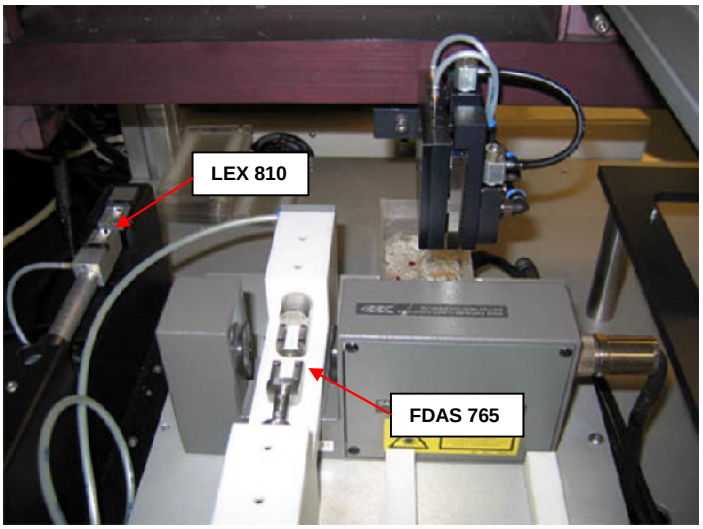

Figure 2.11 Dia-stron® system with FDAS 765 and LEX 810

Dimensional readings from the FDAS 765 laser scan micrometer can be used to demonstrate the diameter distribution among a bundle fibers and along a single fiber. They can also be plotted to show a 3-Dimensional image of the carbon fibers. Each fiber is scanned from 0-180° and rotated by 20° for each measurement. The 180° rotation allows the fiber cross-sections to be characterized due to axial symmetry and plotting the half-diameter (radius) measurement at each 20° rotation for 360° produces the 3D image for one slice of the carbon fiber. Since the FDAS 765 laser scan micrometer takes 10 slice readings along the length of the fiber each segment must be plotted to give the 3D image for the entire fiber length.

2.4.2 Composite Testing:

Each of the prepared UTSI CFSC panels (**Figure 2.8**) was cut to six rectangular strips (**Figure 2.12**) according to the requirements of the ASTM D 6272 and D 7250 standards. The specimen coupons were placed overnight into an oven at 120°C before testing. The apparent density was first measured and then silver coating was applied on the two ends of the coupons as shown in **Figure 2.12** to measure the electrical resistivity. Flexural properties were determined after the measurement of apparent density and resistivity.

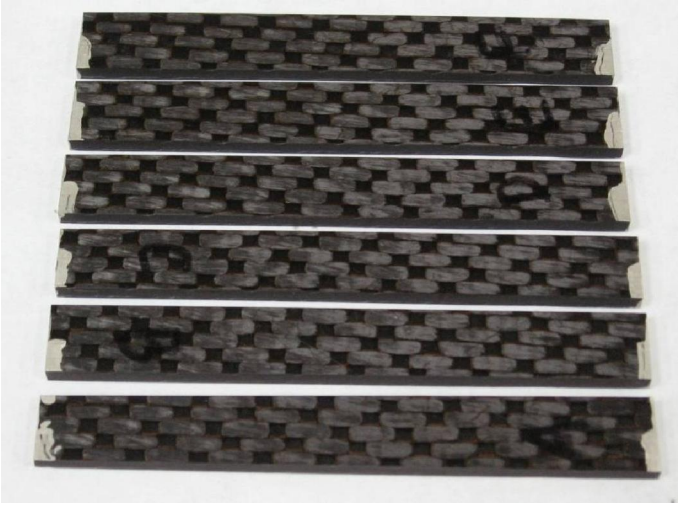

Figure 2.12 Specimen coupons of CFSCs

A. Apparent density and electrical conductivity:

Apparent density and electrical resistivity of CFSCs were calculated by the measurements of mass, dimensions and electrical resistance with a balance, a calibrator, and an electrical bridge, respectively.

B. Flexural strength and modulus (4-point bending):

The flexural strength and modulus of the CFSCs were tested in an MTS machine with a 550 kN load cell and a head speed of 0.1 inch per minute. A precision extensometer was used to measure strain. ASTM D 6272 standards (4-point bending) were used as guides for the testing and calculations. The detail experimental can be seen from Matthew P. Duran's thesis [18].

C. Sandwich beam flexure stiffness (3-point) tests:

The flexural stiffness was also measured in this study to better understand the advantages of the CFSC. Flexural stiffness is the capacity of a structural member to resist bending. The greater the flexural stiffness, the greater the load required to produce a given defection. In terms of the simple beam (the 3-point mid-span deflection of a beam with identical facings in flexure) illustrated in **Figure 2.13**.

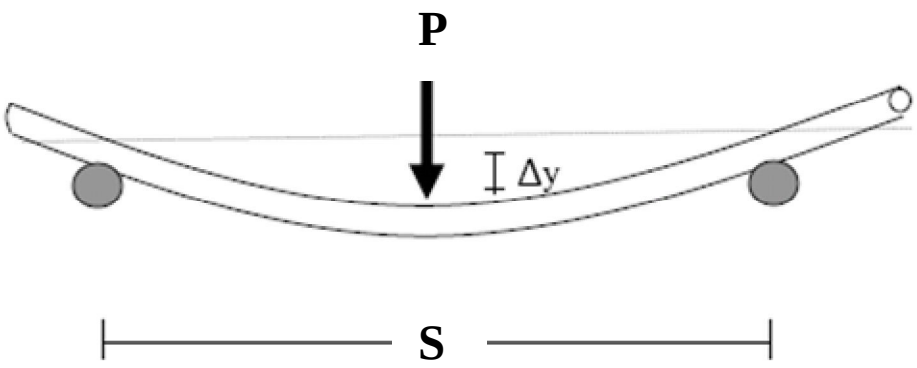

Figure 2.13 3-point mid-span deflection of a CFSC beam

ASTM D 7250 (standard practice for determining sandwich beam flexural and shear stiffness) was used to measure the flexural stiffness, ***D***, the transverse shear rigidity, ***U***, and the core shear modulus, ***G.***

Given deflections and applied forces from results of testing the same sandwich beam with two different loading configurations, ***D*** and ***U*** could be determined from equations (**Eqs 1 and 2**) listed in ASTM D 7250 for the two loading cases., ***G*** could then be calculated using **Eq 3** listed in ASTM D 7250. Due to the length of the equations, the solution for the general loading configuration case is not given here. The following subsections give the solution for common combinations of loading conditions.

$$D = \frac{P_1 S_1^3 (1 - S_2^2 / S_1^2)}{48\Delta_1 (1 - P_1 S_1 \Delta_2 / P_2 S_2 \Delta_1)} \quad (1)$$

$$U = \frac{P_1 S_1 (S_1^2 / S_2^2 - 1)}{4\Delta_1 ((P_1 S_1^3 \Delta_2 / P_2 S_2^3 \Delta_1) - 1)} \quad (2)$$

$$G = \frac{U(d - 2t)}{(d - t)^2 b} \quad (3)$$

Where:

Δ = beam mid-span deflection, mm [in.],

P = total applied force, N [lbf],

d = sandwich thickness, mm [in.],

b = sandwich width, mm [in.],

t = facing thickness, mm [in.],

S = support span length, mm [in.],

G = core shear modulus, MPa [psi],

D = flexural stiffness, N-mm^2 [lb-in.^{2}], and

U = transverse shear rigidity, N [lb].

2.4.3 Optical Microscope:

Fibers must be carefully prepared before they can be observed under the optical microscope. UTSI carbon fibers have many kinks and poor fiber alignment, the crucial step in preparation of embedded samples is to align the fiber.

A new method was developed and is shown in **Figure 2.14**. First, relatively straight portions of fibers are selected from a batch of fibers for each individual method. Then this portion is cut out and wrapped with a short piece of clear vinyl tubing in **Figure 2.14** (A) and (B) then vinyl tubing is tapped up as shown in **Figure 2.14** (C). Epoxy resin made with 5:1 ratio of West Epoxy 105 and West Hardener 206 is then injected into the tubing via a syringe as shown in **Figure 2.14** (D). After the epoxy resin curing the tubing is then peeled open to release the fiber sample now embedded in epoxy shown in **Figure 2.14** (E). The fiber epoxy samples are then arranged in an orderly fashion and placed into an open cylinder shown in **Figure 2.14** (F) where axes of the samples are aligned with the axis of the cylinder in **Figure 2.14** (G).

Epoxy resin with 5:1 ratio is then also poured into the open cylinder to hold all the different samples in place. After polymerization the clear epoxy piece is then taken out of the open cylinder and undergoes polishing with the finished sample shown in **Figure 2.14** (H). Once the epoxy piece is polished then it can be placed under the Optical

microscope for observation and imaging of the individual cross-sections of fibers bundles.

The Optical microscope Olympus® BX60M was used in conjunction with the camera Infinity 1 (**Figure 2.15**) and software Infinity Analyze version 5.0.2 by Lumenera® Corporation to capture images of the carbon fiber cross-sections. Images can be viewed live via the Infinity Analyze software and when suitable captured. Certain images were treated with the flat-field correction to accentuate the Pac-man features.

The flat-field correction compensates for the different dark currents and gains in a detector, in this case the Infinity 1, by creating a uniform output from a uniform signal. **Figure 2.16** demonstrates the difference between a flat-field corrected picture vs. the original. Notice how the flat-field correction changes the background to a uniform grey color, outlines the carbon fibers, and accentuates Pac-man structures.

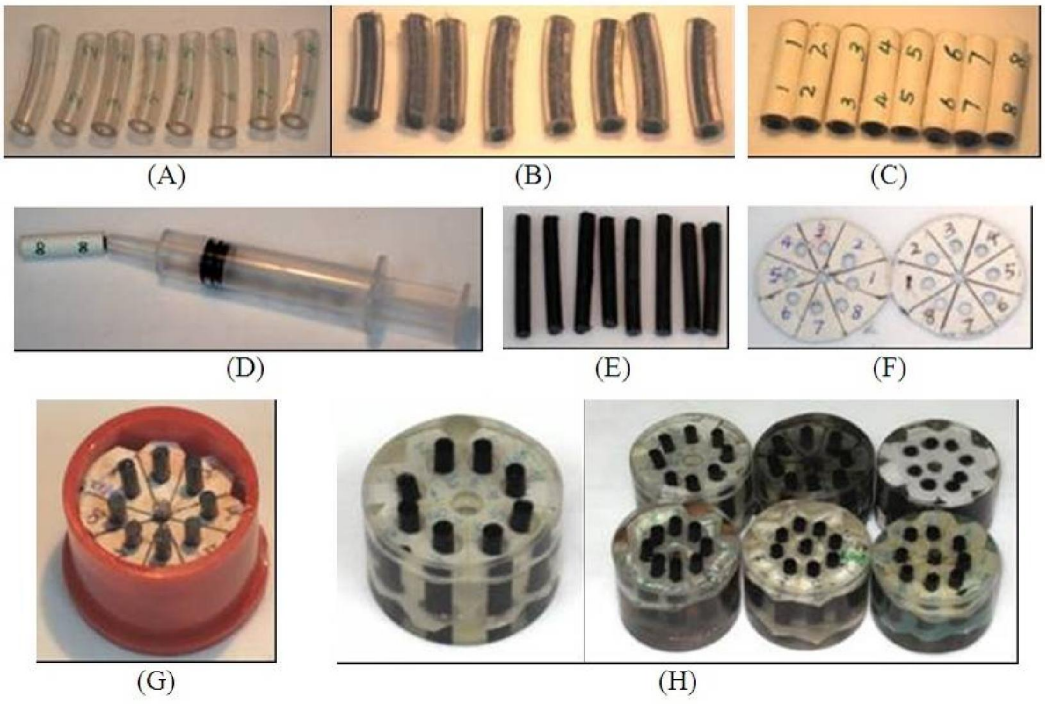

Figure 2.14 Embedded sample preparation

Figure 2.15 Olympus® BX60M and Infinity 1 camera

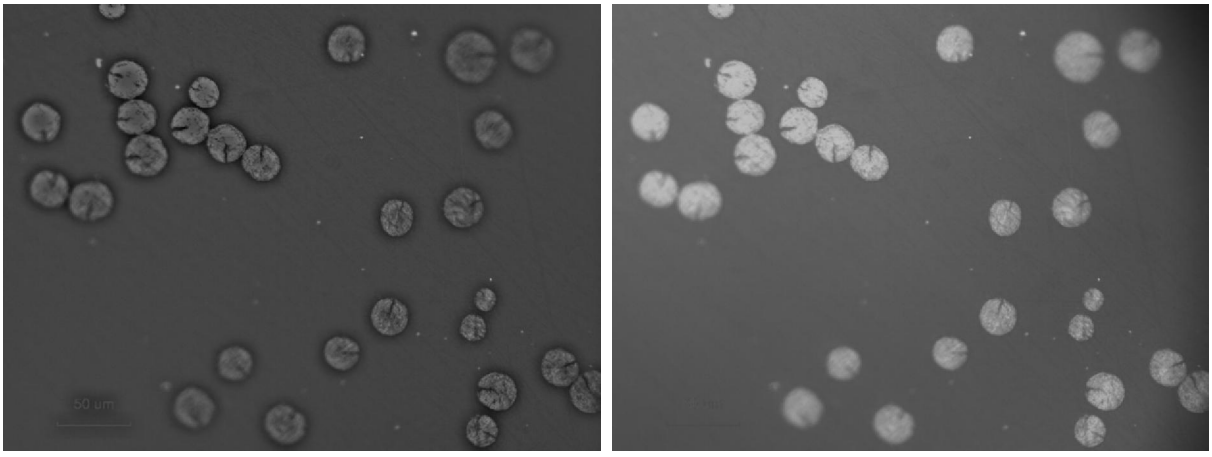

Figure 2.16 Flat-field correction (left) and original image (right)

2.4.4 Image Analysis:

Image analysis was done via a freeware called ImageJ offered by the National Institute of Health (http://rsbweb.nih.gov/ij/). Three critical metrics for optical images of carbon fiber cross-sections are the diameter, cross-sectional area, and the angle of existing Pac-man structures. Cross-sectional area and the fiber diameter can be assessed with the "analyze particle" feature under Analyze in ImageJ but the image has to meet certain requirements before the tool can be utilized.

Measurements of concern must be reported by selecting Analyze à Set Measurements and then selecting "Area", "Shape Descriptors", and "Feret Diameter" (**Figure 2.17** (C)). The image must be pixel scaled so that the measurements correlate to the scale on the image. This is done by drawing a straight line tracing the micron marker on the image (**Figure 2.17** (A)) and then selecting Analyze à Set Scale and then setting it to the known distance which is 50 µm in this case.

The original image shown in **Figure 2.17** (A) must be converted to grey scale if it is not already in grey scale by selecting menu Image à Type à 8 bit. Then the image must be inverted by selecting the menu Edit à Invert. After the inversion the image must then be adjusted so that it is only black and white and this is done by menu Image à Adjust à Threshold. The amount of adjustment should be done in such a way that there are no black dots on the resulting image but it should not subtract so much as to make the cross-sectional areas dramatically smaller than the original image which would result in inaccurate measurements (**Figure 2.17** (B)).

When the threshold adjustment is complete the image can finally be analyzed by selecting Analyze à Analyze Particles. The appropriate settings are shown in **Figure 2.17** (D) for this image. User can adjust the size and circularity for various images but "Show: Outline", "Display Results", "Exclude on Edges", and "Include Holes" must be selected in order to see the full results. Results include "Area" and "Feret" which represents the cross-sectional area and the diameter corresponding to the various carbon fibers shown (**Figure 2.17** (E)) with the outline view (**Figure 2.17** (F)).

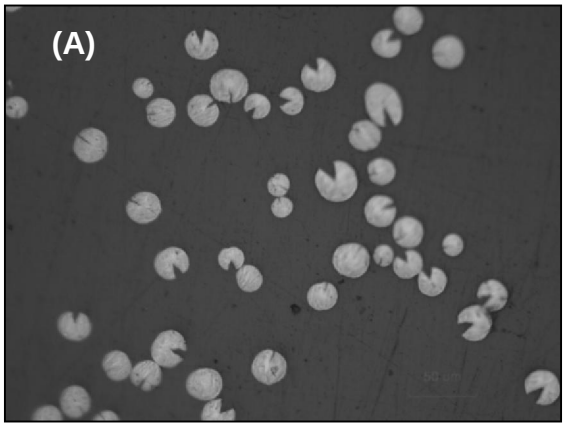

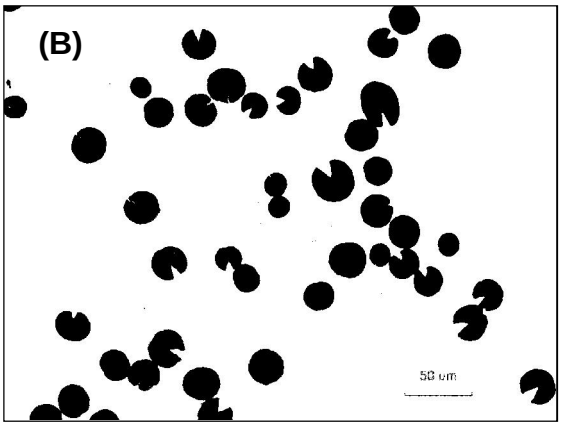

(C)

Set Measurements

☑ Area	☐ Mean Gray Value
☐ Standard Deviation	☐ Modal Gray Value
☐ Min & Max Gray Value	☐ Centroid
☐ Center of Mass	☐ Perimeter
☐ Bounding Rectangle	☐ Fit Ellipse
☑ Shape Descriptors	☑ Feret's Diameter
☐ Integrated Density	☐ Median
☐ Skewness	☐ Kurtosis
☐ Area Fraction	☐ Stack Position
☐ Limit to Threshold	☐ Display Label
☐ Invert Y Coordinates	☐ Scientific Notation

Redirect To: None

Decimal Places (0-9): 3

OK Cancel

(D)

Analyze Particles

Size (micron^2): 10-Infinity

☐ Pixel Units

Circularity: 0.50-1.00

Show: Outlines

☑ Display Results	☑ Exclude on Edges
☐ Clear Results	☑ Include Holes
☐ Summarize	☐ Record Starts
☐ Add to Manager	

OK Cancel

(E)

Results

File Edit Font

	Area	Circ.	Feret	FeretAngle	MinFeret
1	371.600	0.726	23.153	160.313	21.571
2	434.840	0.594	25.908	147.291	22.956
3	506.960	0.891	26.407	68.682	24.769
4	489.960	0.673	26.644	54.162	25.121
5	598.680	0.736	29.424	159.717	25.928
6	197.960	0.868	17.311	130.314	15.132
7	13.280	0.549	6.896	106.858	3.274
8	298.680	0.638	22.064	98.865	18.514
9	290.160	0.644	21.095	137.690	18.889
10	450.800	0.716	25.840	142.864	22.545
11	402.320	0.831	23.532	148.201	22.235
12	547.240	0.839	27.400	50.034	26.078
13	365.200	0.880	22.472	147.724	21.248
14	709.040	0.619	32.703	162.562	30.655
15	449.440	0.535	33.991	96.080	17.475
16	506.040	0.651	27.742	174.207	24.600

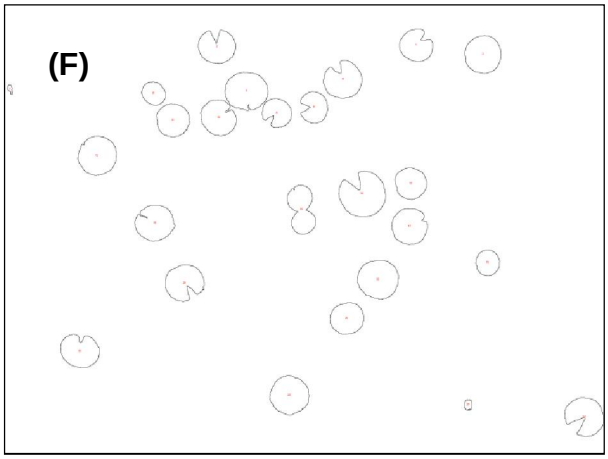

Figure 2.17 "ImageJ" analyze particle procedure

Angle measurement can be taken with the “Angle tool” from the toolbar (**Figure 2.18** (A)). Three points must be selected to measure out the angle of interest (**Figure 2.18** (C), (D)). Selecting Analyze à Measure will display the results (**Figure 2.18** (B)) with “Angle” which corresponds to the angle of the particular Pac-man structure.

2.4.5 SEM:

Scanning Electron Microscope (SEM) was used to observe the microstructure and morphologies of carbon fibers. Carbon fiber samples were sputter coated with a thin layer of gold and then observed with an ISI Super IIIA SEM operated at 10 kV.

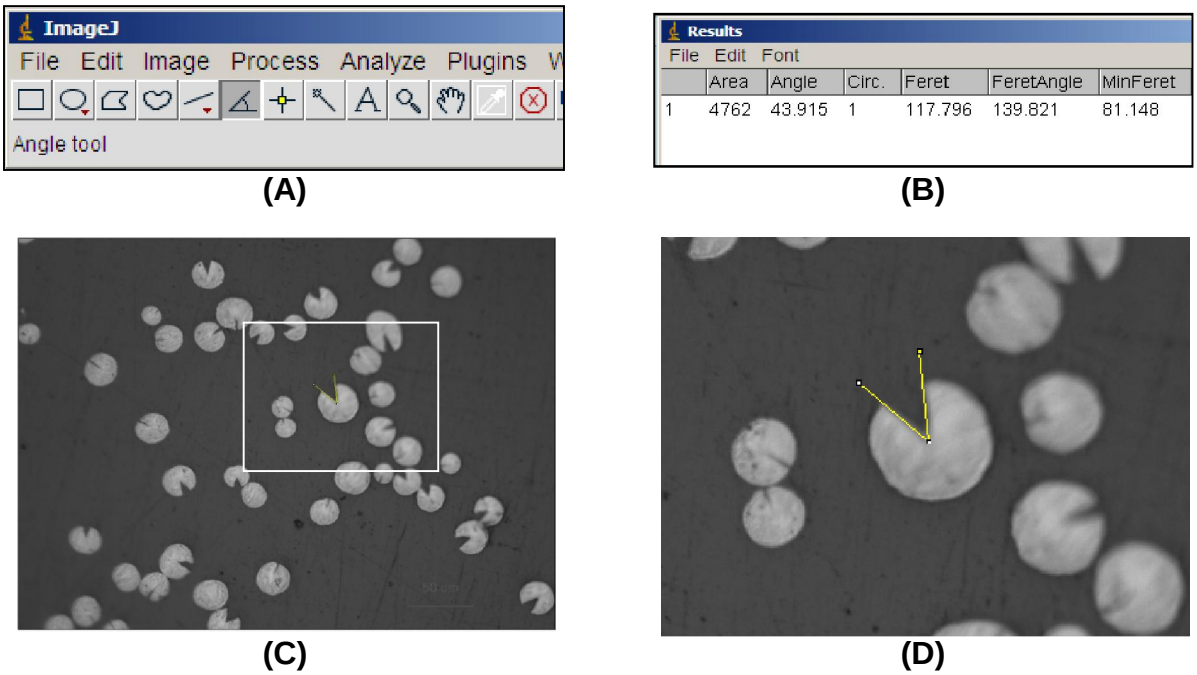

Figure 2.18 “ImageJ” angle measurement

Chapter 3: Influence of Thermal Processes on Structure and Properties of Carbon Fibers

Thermal processes are important steps for making high performance carbon fibers. They influence the structure and properties of the resulting carbon fibers. This chapter will be concerned with the study and understanding of the effect of thermal processes on the structure of stabilized and the resulting carbon fibers. Analysis of the structural difference between fibers and fiber mechanical properties will be also explored to understand their relations.

3.1 Fiber Yields:

Four pitch fibers spun using different blowing speeds were stabilized using the NS method and carbonized at same conditions with the fiber yields shown in **Figure 3.1**. UTSI's pitch-based stabilized fibers show < 5 wt% weight loss as compared to green fibers.

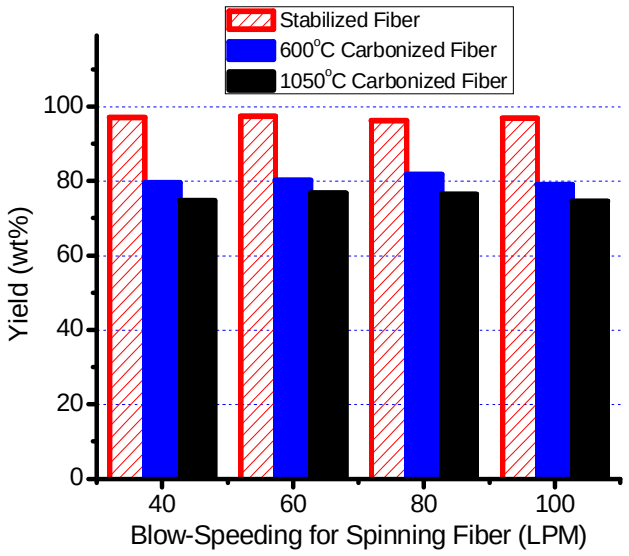

Figure 3.1 Yields of fibers after stabilization and carbonization at lower (600°C) and higher (1050°C) temperatures

It was reported that the green fibers spun from solvated mesophase pitch contain ~ 12 wt% solvents [19]. Most of solvents in the fiber are removed and fiber undergoes weight loss during the stabilization process done with air from 150 to 350°C. During the stabilization process, the fiber will be oxidized (introduction of oxygen) and gain weight.

After the stabilization process, the stabilized fibers are carbonized in N_2 at higher temperatures to remove all other non-carbon elements. The carbonized fibers show a weight loss of ~ 20 wt% at 600°C and ~ 25 wt% at 1050°C respectively. With approximately 75% (even higher at ~ 87% if disregarding the solvents) carbon yield as compared to the 50-55% carbon yield of PAN fibers [20].

3.2 Fiber Diameter:

Fiber diameter also changes with thermal processes. **Figure 3.2** shows the fiber diameter reducing from stabilized fiber to carbonized (low and higher temperature) fibers.

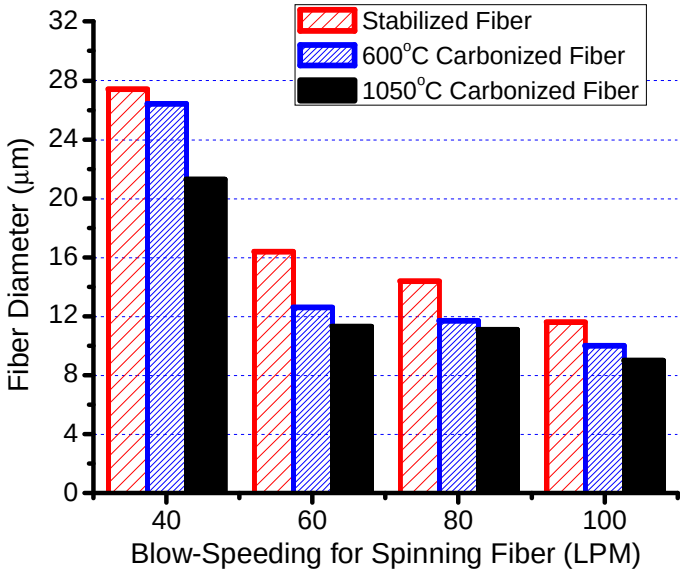

Figure 3.2 Diameter of fibers after stabilization and carbonization at lower (600°C) and higher (1050°C) temperatures

The optical microscope images shown in **Table 3.1** display the obvious difference between green and carbon fibers. Higher blowing speeds of 100 LPM produced green fiber with smaller diameter leading to a smaller (~ 9 μm) diameter carbon fiber. It was found that the diameter of green fiber does not change distinctly after stabilization under normal levels but there are distinct changes during the carbonization process. The reduction in diameter is the result of radial shrinkage of fiber due to chemical reactions such as cross-linking and aromatic reaction. From **Table 3.1** it can be seen that carbon fiber with a larger diameter usually presents a radial crack structure or a “pac-man structure”.

3.3 Evolution of Fiber Structure:

The appearance of pac-man structure in the carbon fiber (**Table 3.1**) led to a research focusing on the development and evolution of pac-man structures during the thermal processes. Larger diameter green fiber spun with lower blowing speed at 40 LPM was chosen as a precursor fiber for the investigation of pac-man structures. The fiber was stabilized with 2S2 method. The stabilized fiber was then carbonized in N_2 at various temperatures from 400-1000°C in 100°C increment. Eight samples, including stabilized fiber, were observed using an optical microscope as shown in **Figure 3.3** with flat-field correction.

Formation of pac-mans in stabilized fibers is not readily detectable or as apparent compared to the carbonized counterpart. The pac-man structures start to reveal themselves starting from 600°C. They become distinctly noticeable at 700°C as seen with the fiber at the center of the picture. From 800°C and onwards the pac-man structures can be observed in almost every fiber with the angle of the pac-man mouth being the greatest at 1000°C.

The high magnification images obtained from SEM shown in **Figure 3.4** displays the pac-man structure development along the fiber axis.

Table 3.1 Diameter of green fiber vs. carbon fibers

LPM	Green Fiber	NS (1050°C) - Carbon Fiber
40	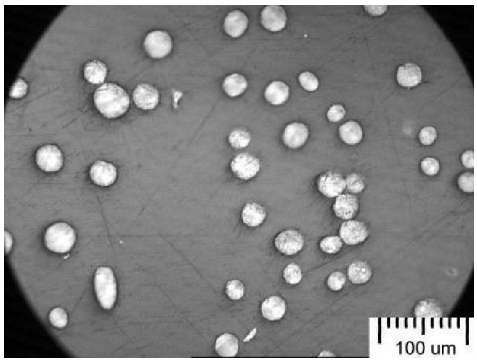	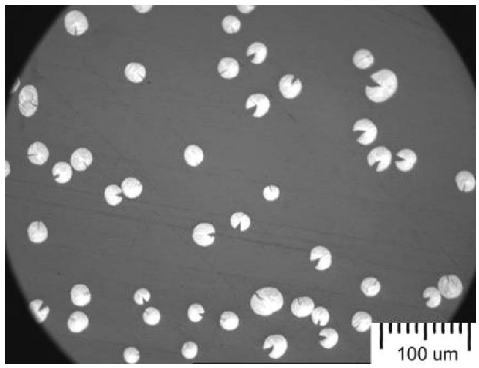
60	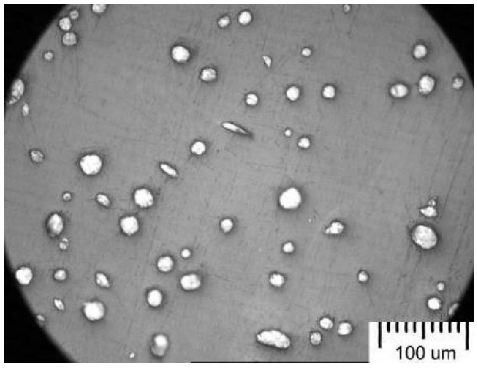	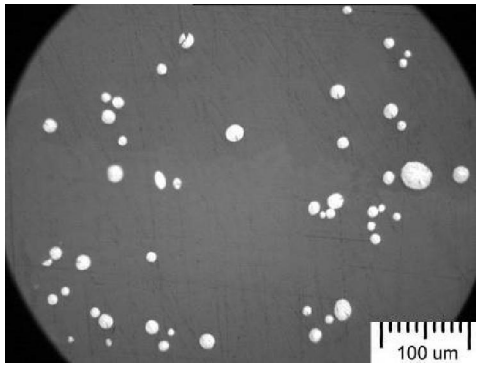
80	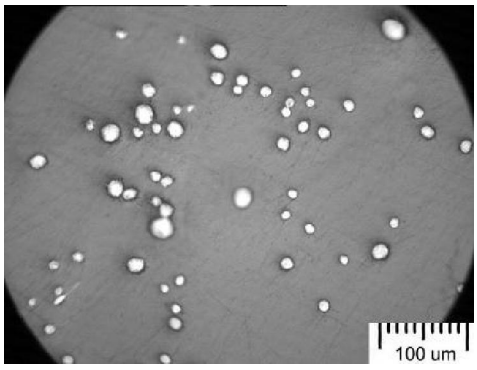	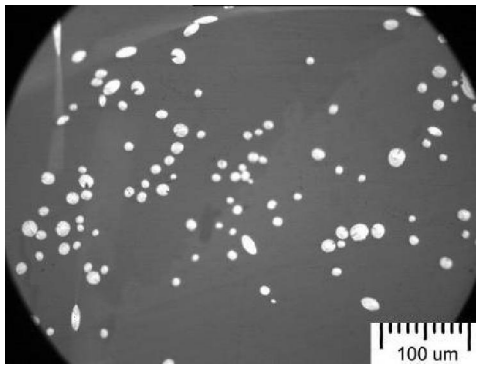
100	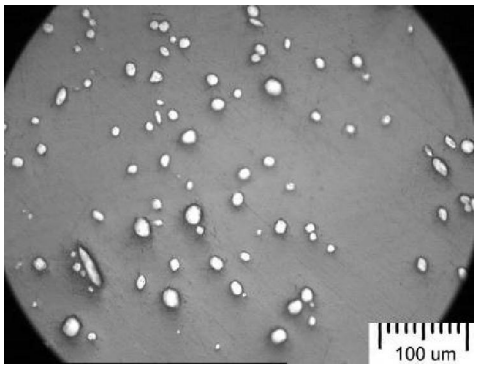	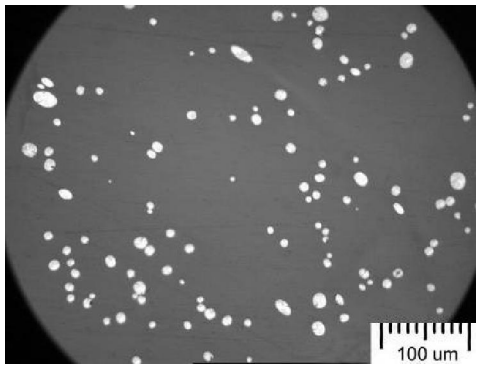

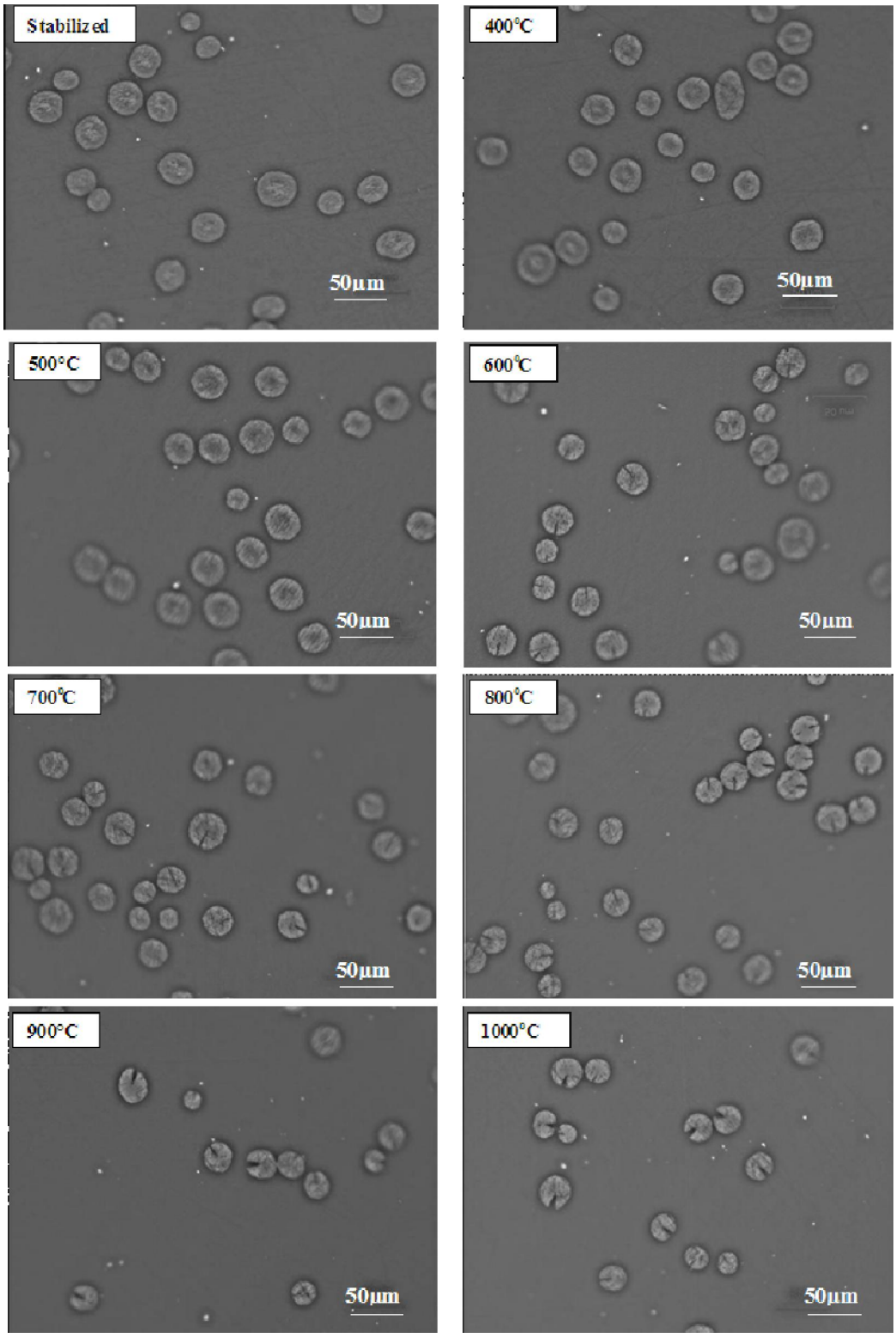

Figure 3.3 Development of pac-man structure during carbonization

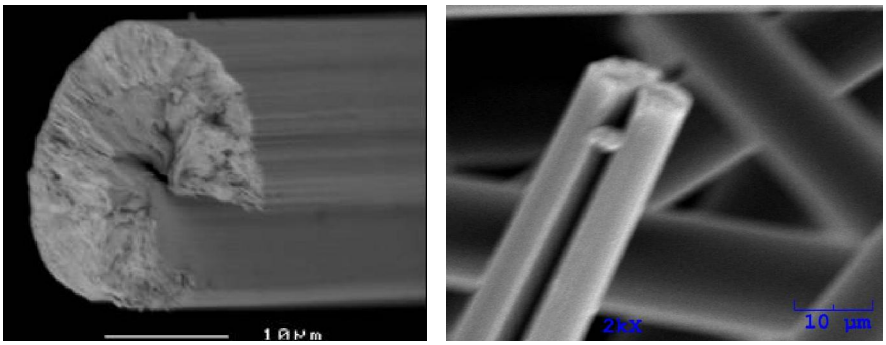

Figure 3.4 SEM images showing pac-man structure of carbon fibers

3.4 Effect of Stabilization Conditions on Fiber Structures:

The results from the above studies indicate that the pac-man structure was developed in the larger diameter fiber carbonized at lower temperature of ~ 600°C and several questions were raised. Why does the pac-man structure formed more often in larger diameter than in smaller diameter fiber? Does the stabilization process affect fiber structure? To answer these questions, green fibers were stabilized with various stabilization and carbonization processes. The structure of stabilized fibers and the resulting carbon fibers were investigated with the optical microscope and SEM.

3.4.1 Stabilized Fiber:

Figure 3.5 shows optical microscope images of Normal Stabilization (NS) stabilized fibers which were oxidized from green fibers (see **Table 3.1**) spun at 40 and 100 LPM, respectively. From **Table 3.1** no special features were found in green fibers except the fiber diameter decreased with increasing blow speed from 40 to 100 LPM. However, after stabilization sheath-core structures were observed in larger diameter stabilized fibers (see arrows in **Figure 3.5**) from most 40 LPM fibers and only one large fiber in 100 LPM. Sheath is believed to be composed of well-stabilized, cross-linked, and relatively hard material while core is composed of less-stabilized and relatively soft material. When the fiber embedded in epoxy resin was polished, the fiber cross-sectional surface may not be flat due to the sheath-core structure as shown in **Figure 3.6**. The center (core) of the fiber is lower than the edge (sheath) which is one explanation for a two-phase structure observed under optical microscope.

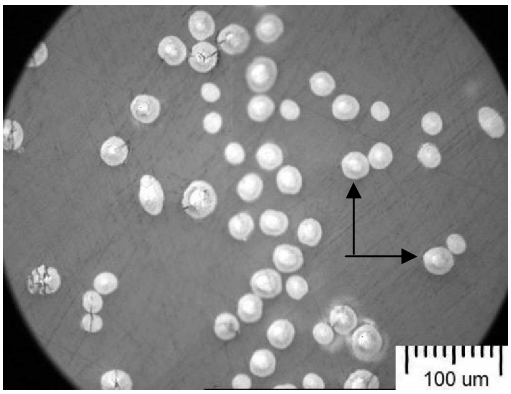

40 LPM

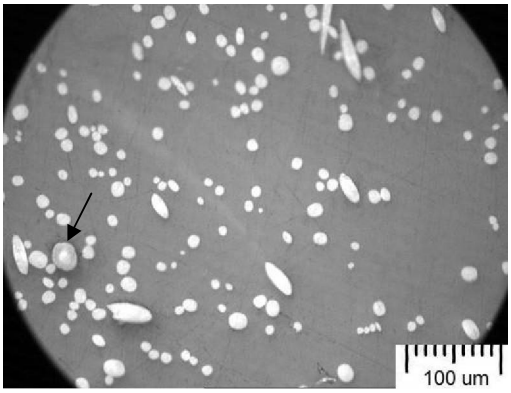

100 LPM

Figure 3.5 Optical microscope images of stabilized (NS) fibers

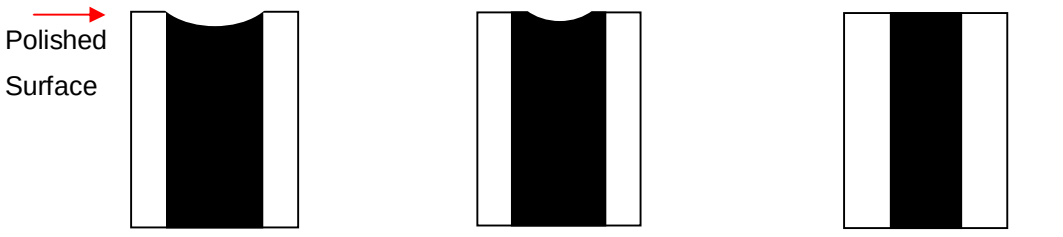

Green fiber

stabilized fiber with larger diameter

stabilized fiber with small diameter

Figure 3.6 Possible condition of embedded sample's polished fibers

This result suggests that the stabilization of the green fiber is controlled by the diffusion of oxidation from outside layer to internal core. Thus, small diameter fiber is easy to be stabilized uniformly, but larger diameter fiber may stabilize gradually resulting in sheath-core structure. Stabilization conditions including temperature, time, multi-steps will definitely affect the sheath-core structure of stabilized fibers which may also determine the structure and properties of the resulting carbon fibers.

3.4.2 Carbonized Fiber:

Stabilized fibers that exhibited a sheath-core structure evolved to pac-man structures in the carbon fiber counterpart as witnessed in NS shown in **Table 3.1**. Other examples for the relationship between sheath-core structure of stabilized fiber and pac-man structure of the resulting carbon fiber are shown in **Table 3.2** and **Table 3.3**. As compared with fibers of same (40 LPM) spinning speed, multi-level 4S2 (**Table 3.2**) stabilized fiber has a smaller core area than NS stabilized fiber (**Figure 3.5**). The resulting 4S2 carbon fibers display less pac-man structures with smaller pac-man angles because of a smaller core. In the case of Long Stabilization (LS) (**Table 3.3**), sheath-core structures are non-existent for stabilized fibers and the resulting carbon fibers do not show any pac-man structures.

However, if the green fiber was stabilized under a very Short Stabilization (SS) time (see **Table 3.4**), the sheath-core structure of the stabilized fiber is difficult to observe due to a very thin sheath. SS fibers are carbonized directly at a high temperature and the non-stabilized core melts to form a hollow core in the resulting carbon fiber. SEM images, shown in **Figure 3.7**, reveal the formation of hollow carbon fibers. The hollowed carbon fiber may find application in the area of light-weight composites, carbon fiber membrane, functional fiber, and highly porous fiber after activation.

In summary, the stabilization condition has a strong effect on formation of the sheath-core structure of stabilized fibers and pac-man and hollow structures of the resulting carbon fiber. The mechanism for the relationship between stabilization process and fiber structures can be summarized in **Table 3.5.**

Table 3.2 Sheath-core structure of 4S2 stabilized fibers vs. pac-man structures of the resulting carbon fibers

LPM	4S2 - Stabilized Fiber	4S2 (1050°C) - Carbon Fiber
40	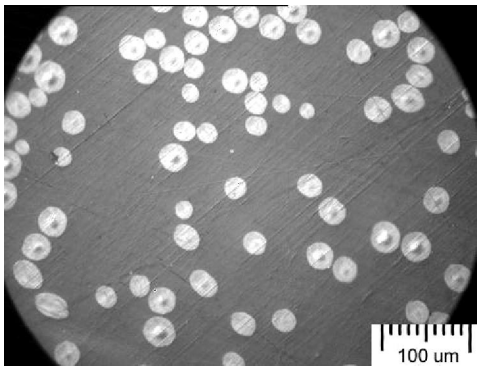	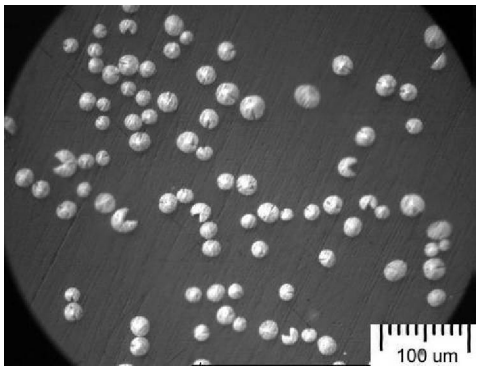
60	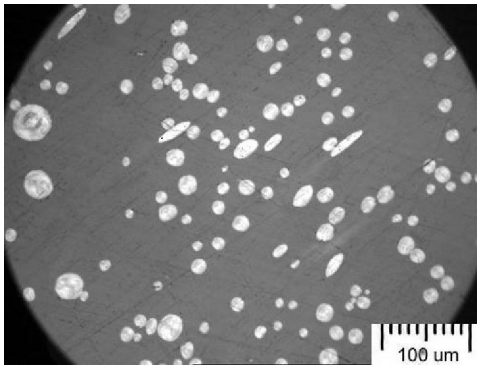	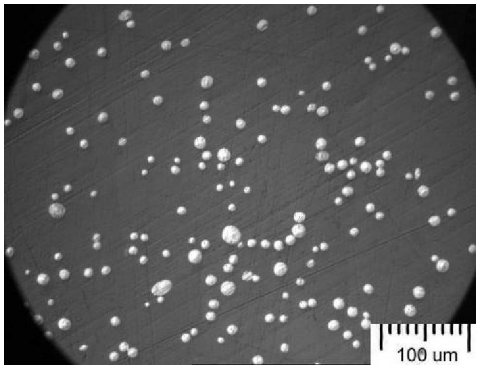
80	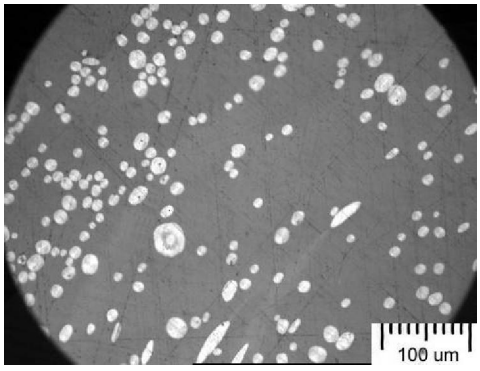	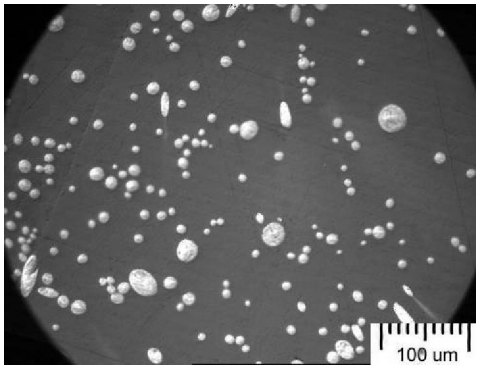
100	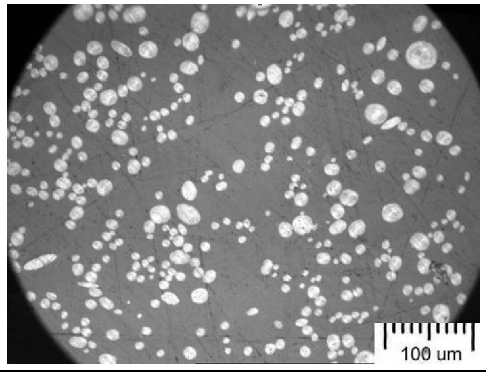	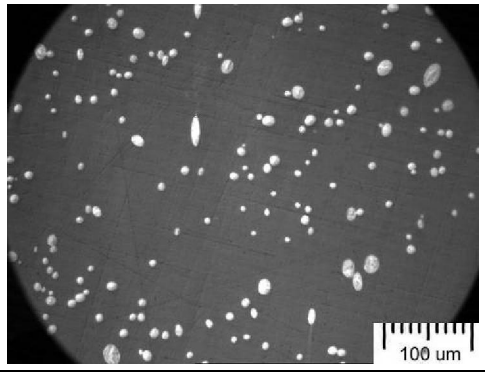

Table 3.3 Long time stabilization resulting in absence of sheath-core and pac-man structures

LPM	LS - Stabilized Fiber	LS (1050°C) - Carbon Fiber
40	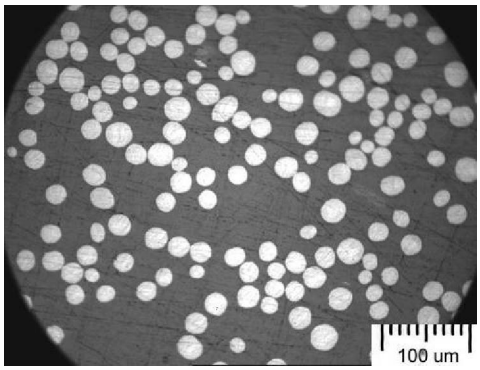	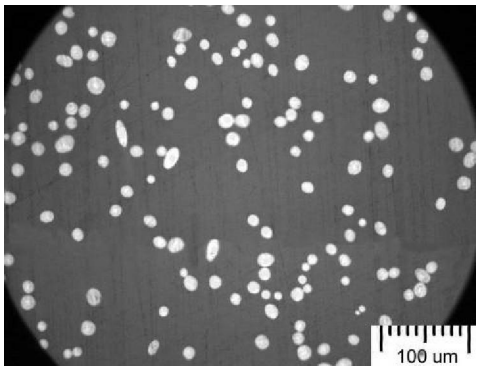
60	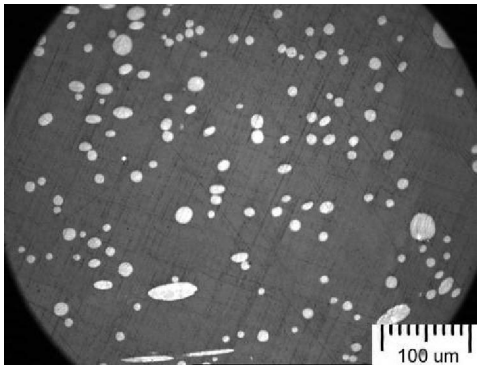	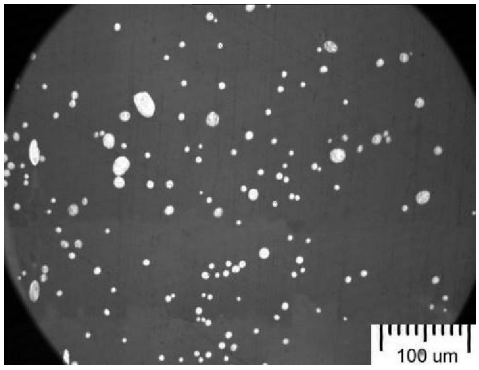
80	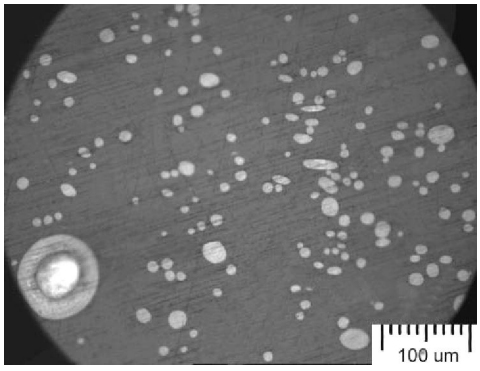	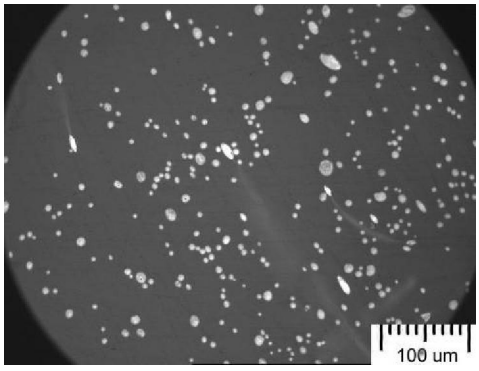
100	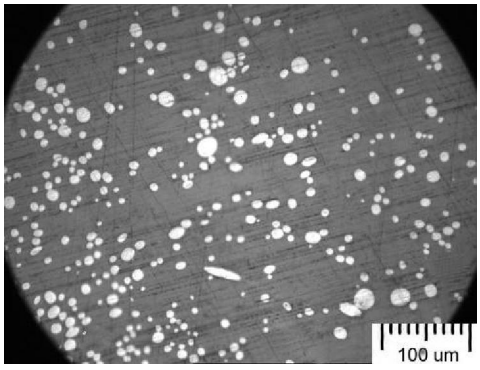	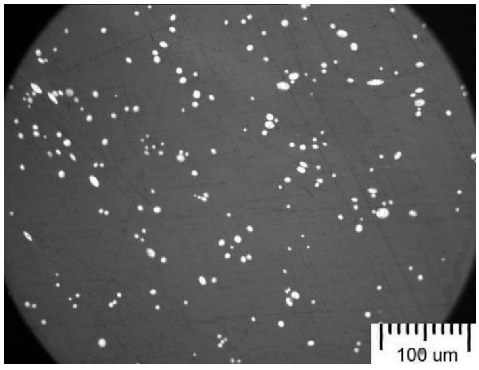

Table 3.4 Very short time stabilization resulting in absence of sheath-core of the stabilized fiber but presence of hollow carbon fiber

LPM	SS - Stabilized Fiber	SS (1050°C) - Carbon Fiber
40	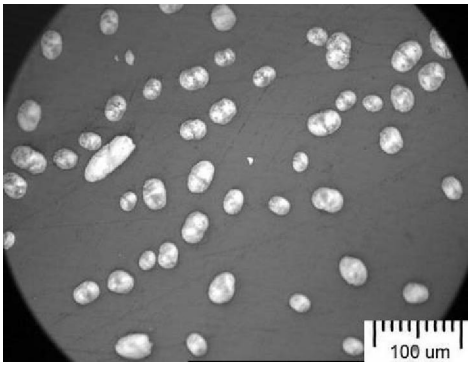	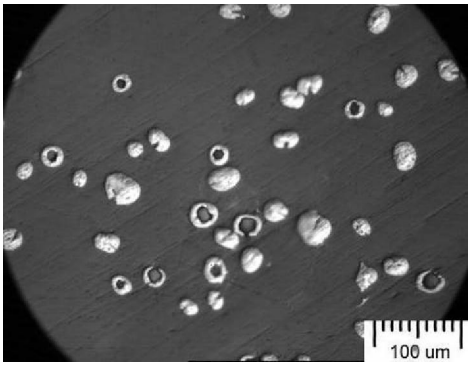
60	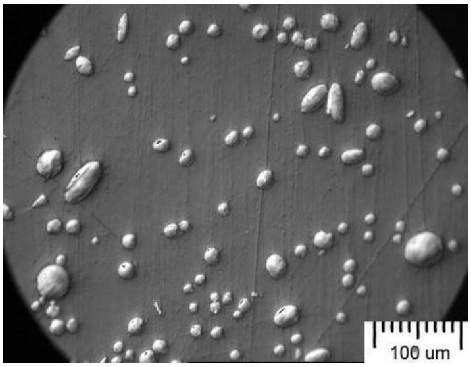	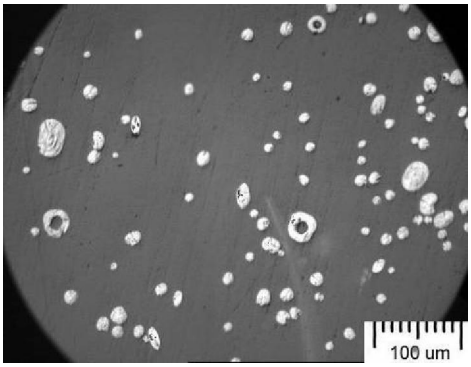
80	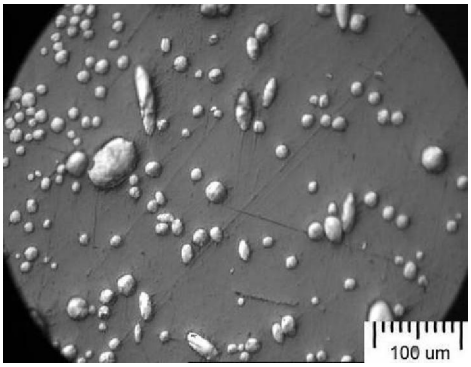	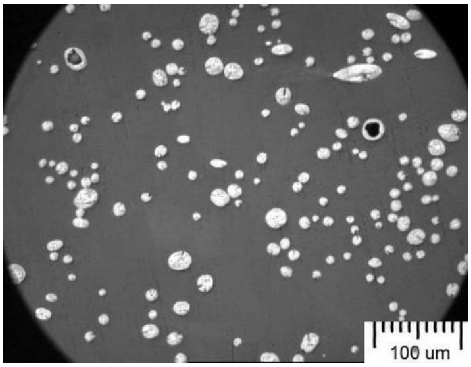
100	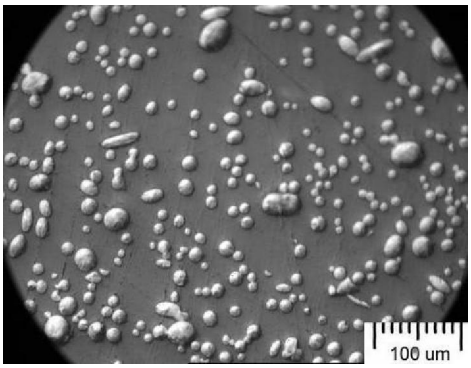	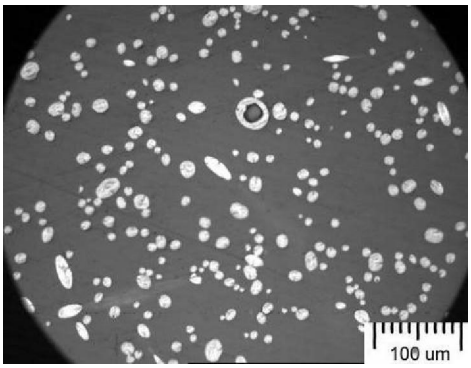

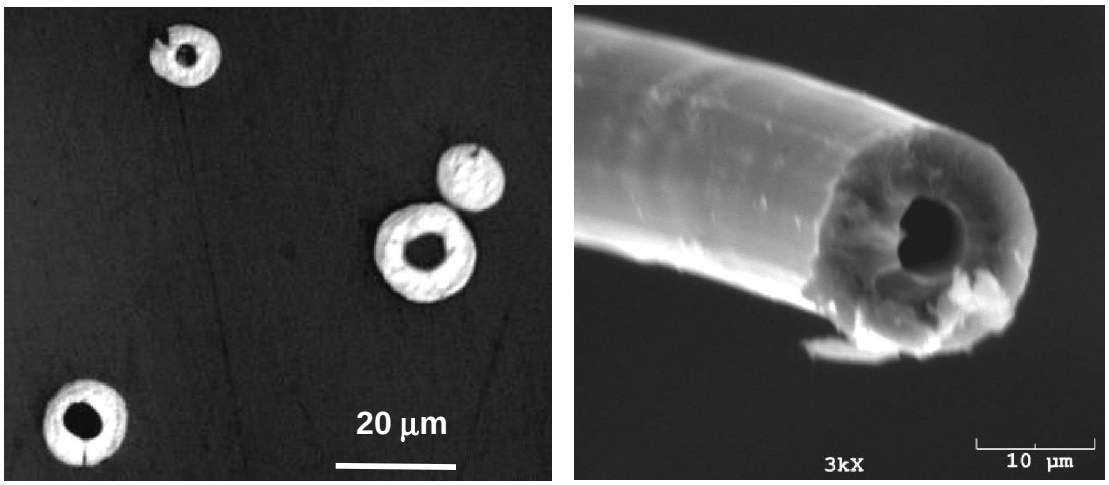

Figure 3.7. Optical (left) and SEM (right) micrographs of the hollow carbon fibers

Table 3.5 Proposed mechanism of the formation of sheath-core, pac-man, and hollow structures depending on the stabilization conditions

Stabilization condition	Green	SS	NS	4S2	LS
Level of Stabilization					
Cross-section of Stabilized Fiber					
Polished status of Stabilized fiber in epoxy					
Cross-section of Carbon fiber					

3.5 Effect of Stabilization Conditions on Properties of Carbon Fibers:

Mechanical properties of carbon fibers depend on many variables such as precursor materials, fiber spinning, stabilization processes, and carbonization temperatures. Stabilization processes not only affect the structure and properties but also determines the cost of carbon fibers because stabilization processes usually consume longest time in the manufacture of carbon fibers. In this study, to understand the effect of stabilization processes on the properties of UTSI solvated pitch-based carbon fibers, larger diameter green fiber spun at 40 LPM was chosen as precursor fibers for the following research work. 40 LPM fiber forms distinct structure by different stabilization processes as indicated above sections making it ideal for this investigation. Different stabilization methods namely one-step, two-step, and multi-step, combining with same carbonization method, and their effects on the mechanical properties of the resulting carbon fiber were investigated.

3.5.1 One-step Stabilization:

One-step stabilization was carried out by thermally treating green fiber in air at 350°C. Generally, for a regular diameter (< 10 μm) fiber, the stabilization time was setup around 60 min. Based on previous experience, the initial stabilization time was setup for 60 min, and the method was called Normal Stabilization (NS). The stabilization time longer than 60 min was expected for the larger diameter green fiber used in this study.

In this study, the improvement of mechanical properties is more important than the actual values. Low final carbonization temperature (1050°C) used and the large fiber diameter both limit the full potential of the prepared carbon fiber's mechanical properties. All mechanical properties are normalized against NS' fiber properties.

The initial experiment compares LS with NS and the results are shown in **Figure 3.8**. With the stabilization time increased from 60 to 360 min, the resulting carbon fiber shows improvement in both tensile strength and modulus. This suggests that larger diameter green fiber may need longer stabilization time at 350°C to obtain stronger carbon fibers. However, 360 min is too long for stabilization and must be reduced to balance time spent in stabilization with the desired properties.

3.5.2 Two-step Stabilization:

As compared with one-step stabilization which holds the fiber at a constant temperature, two-step stabilization uses two temperatures steps in the stabilization processes. Stabilization of solvated mesophase pitch fiber includes removal of solvents and oxidation reactions which introduce functional groups into the fiber and lead to a subsequent cross-linking of the oxidized pitch molecules. All these reactions could occur at temperatures ranging from 150-450°C. However, each of these reactions requires different temperatures and time to be completed. Stabilization processes with greater than one-step is expected to reduce stabilization time and improve the mechanical properties of the resulting carbon fibers.

In this study, two temperatures of 275°C and 375°C were employed to stabilize the green fibers. The stabilization time is of equal proportions for both temperatures. The total stabilization time is two, three, four, and five hours for methods 2S2, 2S3, 2S4, and 2S5, respectively. The total time is longer than 60 min (NS) but shorter than 360 min (LS). **Figure 3.9** shows the normalized strength and modulus of carbon fibers as a function of total stabilization time. Two-step stabilization results in higher strength and modulus as compared with one-step stabilization NS and LS shown in **Figure 3.8**.

From **Figure 3.9**, the strength increases with increased stabilization time from two to four hours but decreases at five hours (300 min). This suggests that a long time stabilization is not good for carbon fiber strength due to the over oxidation of the green fiber and subsequent formation of structure defects on fiber during the carbonization process.

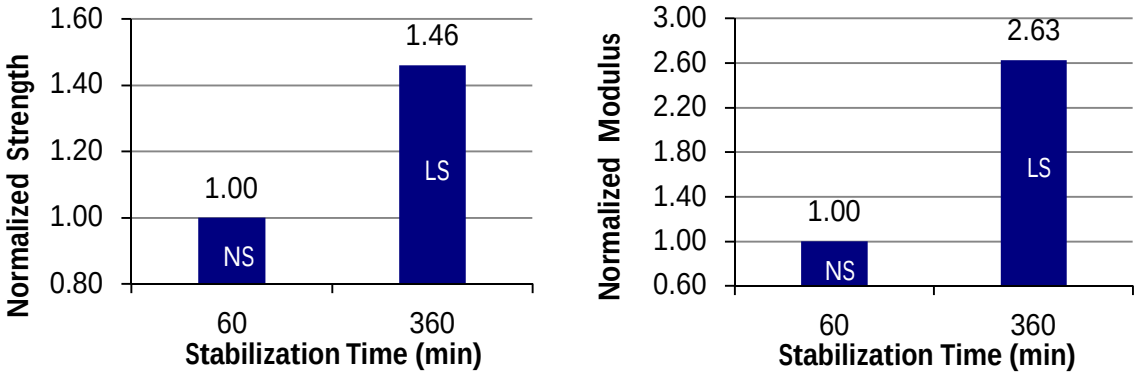

Figure 3.8. Comparison between normal (NS) and long (LS) stabilization

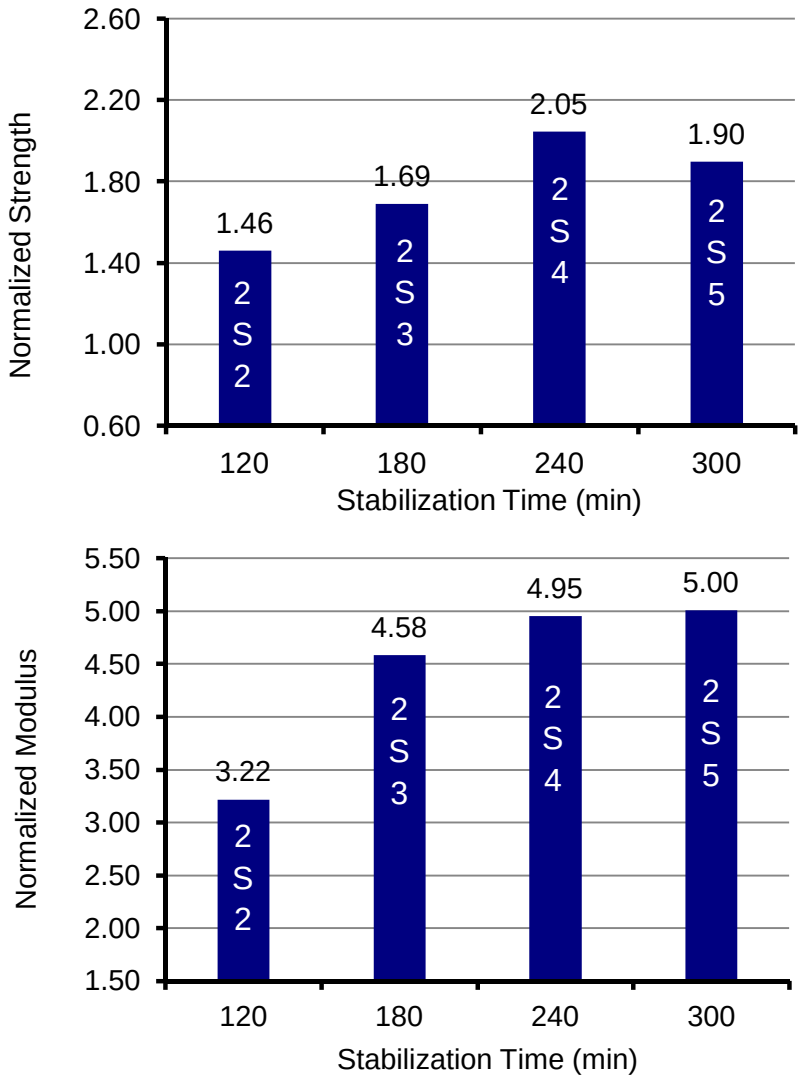

Figure 3.9. Normalized strength and modulus of carbon fibers as a function of total stabilization time in two-step stabilization processes

3.5.3 Multi-step Stabilization:

Since two-step is a promising stabilization method that can reduce stabilization time and improve carbon fiber mechanical properties, a further investigation on multiple (more than two temperature steps) stabilization was carried out and the results are shown in **Figure 3.10**.

At first, a 4-step stabilization (2S2) method was tested. The stabilization conditions were set: 250°C (30 min), 300^{o}C (30 min), 350°C (30 min), and 400°C (15 min). The total time (105 min) is controlled less than 2 hours. As compared with **Figure 3.9**, the normalized strength of 2.48 indicates that 4-step stabilization (4S2) is much better than 2-step stabilization (2S2, 2S3, 2S4, and 2S5) methods.

To investigate the effect of multi-step stabilization, the steps were doubled to see if additional improvements in tensile strength and modulus of carbon fiber can be obtained. Here, a relatively lower temperature (e.g. 230°C vs. 250°C) was chosen based on a literature paper which gave insight into the reactions that occur at lower stabilization temperature regions [21]. Since 4S2 had the most economical mechanical properties for time spent in stabilization multi-step stabilization was set to two hours.

Three 8-step stabilization methods (8S2, LB, and HB) were conducted. 8S2 has same time (15 min) in each of eight temperatures steps. With the two hours constraint LB and HB methods were explored to investigate the effects of a bias temperature profile. LB spends longer time at the lower temperature range and visa-versa for HB.

The results in **Figure 3.10** show LB with a major improvement over other method in tensile strength and modulus. Conversely, HB had the worst tensile strength aside from the initial NS method and the tensile modulus is only a moderate improvement. This suggests that stabilization at lower temperatures for longer time and at higher temperatures for short time may be beneficial to mechanical properties of resulting carbon fibers.

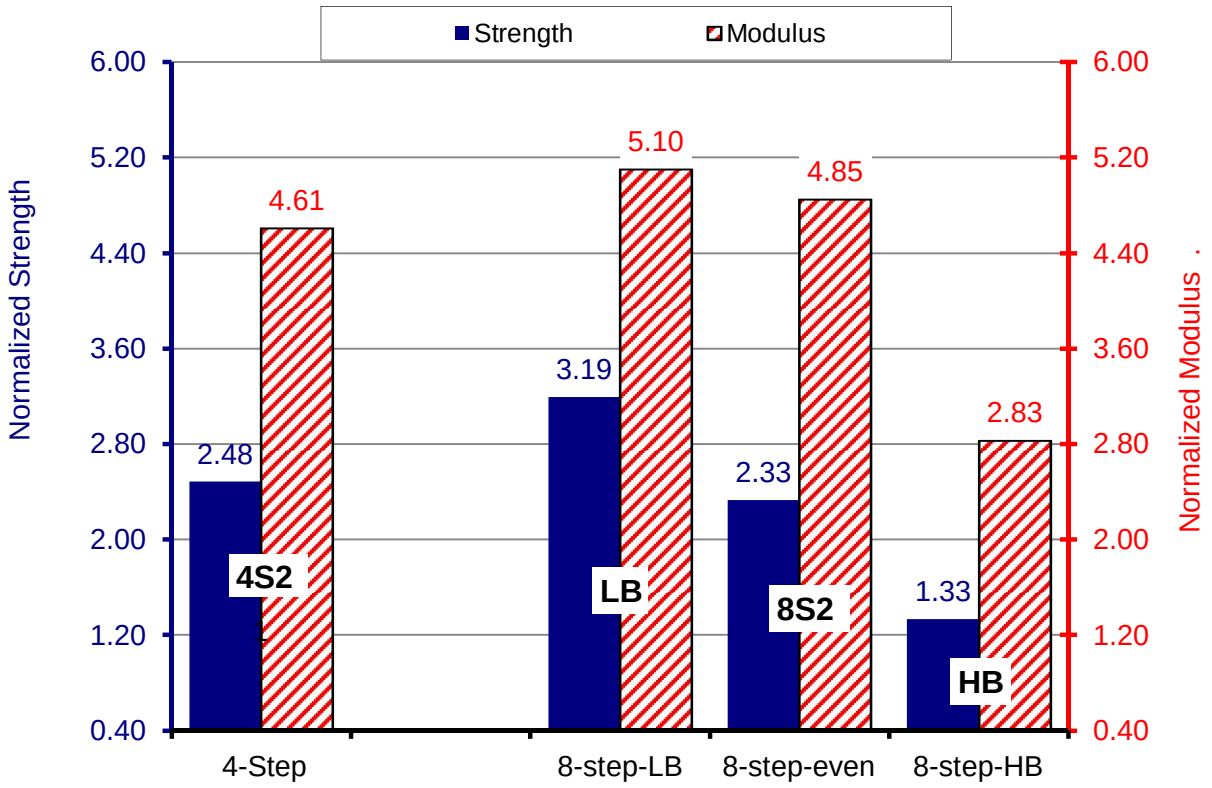

Figure 3.10. Effect of Multi-step stabilization on normalized strength and modulus of carbon fibers

Chapter 4: Measurement and Analysis of Fiber Structure Uniformity

Fiber structure uniformity is of importance to evaluate the quality of carbon fibers and also has influence on the design and final physical properties of the fiber-reinforced composites. In the previous Chapter, optical microscope and SEM pictures revealed fiber diameter non-uniformity and pac-man structure existed in the UTSI carbon fibers. These inspired a systemic investigation of fiber structural features and uniformity. In this Chapter, fiber diameter distribution for a bundle fiber and along a single fiber, 3D plots, and pac-man angle are investigated by using a laser scan micrometer, an optical microscope, and image analysis software.

4.1 Fiber Size Distribution for a Bundle Fiber:

Fiber diameter distribution for a bundle fiber was examined with two different methods at the UTSI. One is single fiber measurement using a laser scan micrometer; another is a bundle fiber embedded in epoxy resin, polished, and then measured using an optical microscope.

4.1.1 Laser Scan Micrometer:

Four UTSI carbon fibers spun through four different blowing speeds and one commercial pitch-based (P-25) and one PAN-based carbon fiber, were employed for fiber size measurement using a laser scan micrometer. The typical fiber diameter distribution, average diameter, and standard deviation measured from 15 single fibers for each of these six carbon fibers are shown in **Figure 4.1.** UTSI carbon fibers present wider diameter distribution than commercial carbon fibers. In the case of UTSI carbon fibers, the larger diameter fiber (40 LPM) displays wider diameter distribution than smaller diameter fiber (100 LPM).

Ten large diameter carbon fibers prepared from same batch of green fiber (40 LPM) but using different stabilization methods were investigated to confirm this diameter

non-uniformity. **Figure 4.2** shows fiber diameter and fiber cross-sectional area with deviation. The diameter distribution resembles the distribution of the cross-sectional area and this is normal because the cross-sectional area is derived from the diameter readings. All the carbon fibers show spread diameter and cross-sectional area distribution (large deviation) due to the nature of the spinning method and the precursor fibers produced at 40 LPM.

It must point out that in despite of laser scan micrometer, which is believed to be an excellent technique for the dimension measurement, there are still drawbacks for current methods for the measurement of fiber diameter and fiber cross-sectional area.

More errors exist for a noncircular fiber and fiber with pac-man structures in the measurement of fiber diameter and cross-sectional area which is used for the calculation of fiber strength and modulus. There is limitation in the number of fibers being measured as each tray holds 15 samples and takes around four to six hours to measure the diameter and perform the tensile test. Fibers are also hand selected ("fiber selective effect") from a bundle fiber for diameter and tensile measurements.

To address these problems, further analysis by optical microscope method was carried out to determine the fiber structure uniformity of a more accurate method.

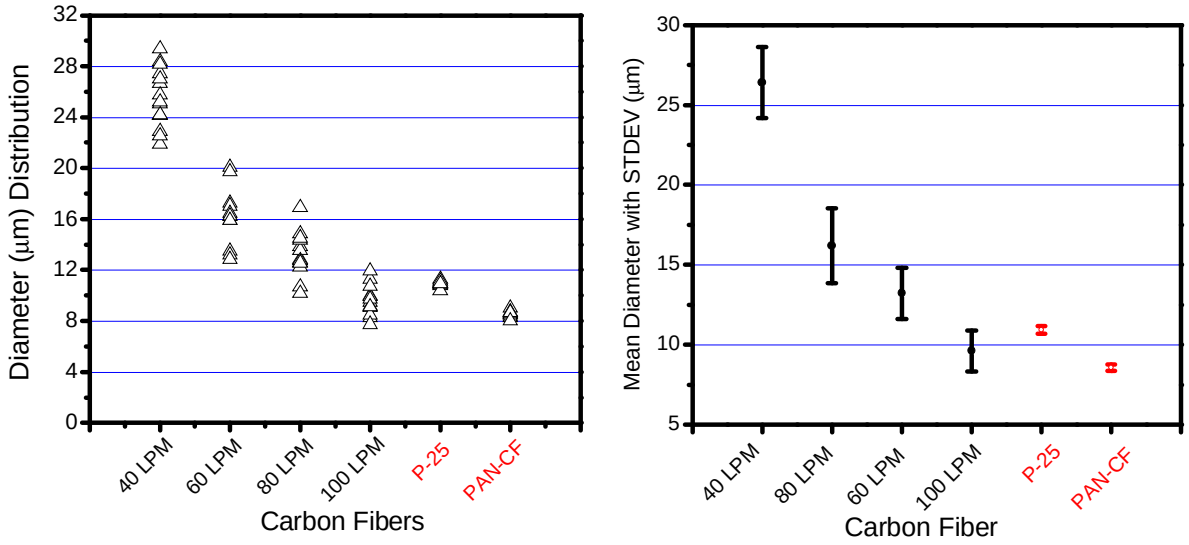

Figure 4.1 Fiber diameter distribution (left) and mean diameter with stdev (right) comparing four UTSI carbon fibers with commercial carbon fibers.

4.1.2 Optical Microscope:

Large diameter (40 LPM) fibers were employed in this study since they displayed large structure non-uniformity. Ten above carbon fibers shown in **Figure 4.2** were also measured using optical microscope method. Pac-man structures can be noted for most of the fibers except LS. The typical images are shown in **Figure 4.3**. It is believed that the cross-section area of the fiber with a pac-man structure could not be measured correctly using a laser scan micrometer.

As compared to laser scan micrometer, optical microscope method allows a large number of single fibers to be examined at the same time and avoids the "fiber selective effect". Thus, this method should give a real statistic value of average fiber diameter and its distribution. In addition, with the help of computer software, fiber cross-sectional area was directly measured so that more accurate results can be obtained for non-circular fiber and fiber with cracks such as pac-man structure.

However, sample preparation is a key point for the optical microscope measurement which has been solved for UTSI carbon fibers. To obtain a right fiber cross-section the fibers in the bundle must be aligned in the embedded sample; the polished fiber surface must be perpendicular to the fiber axis.

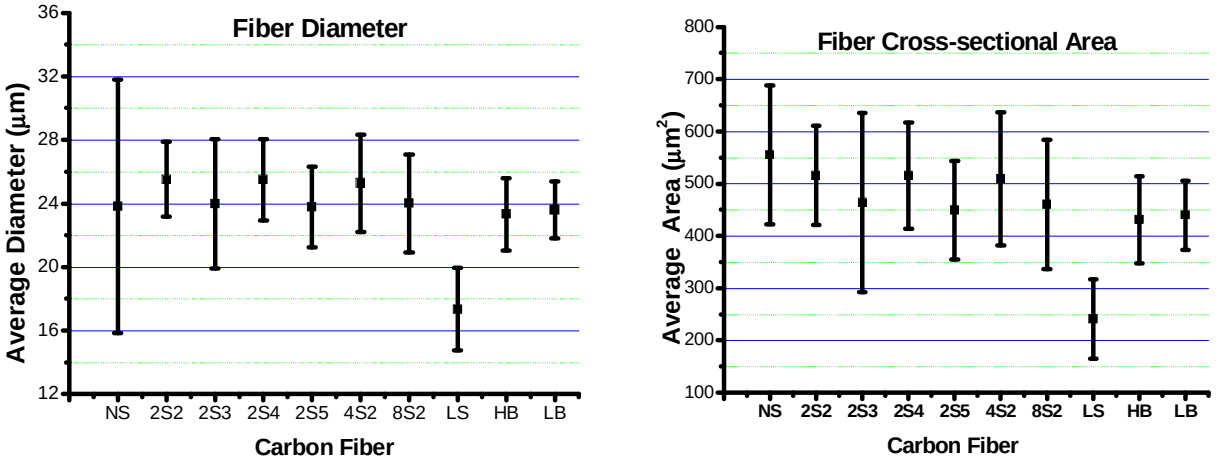

Figure 4.2 Diameter (left) and cross-sectional area (right) measured with laser scan micrometer comparing large diameter (40 LPM) carbon fibers prepared with different stabilization methods

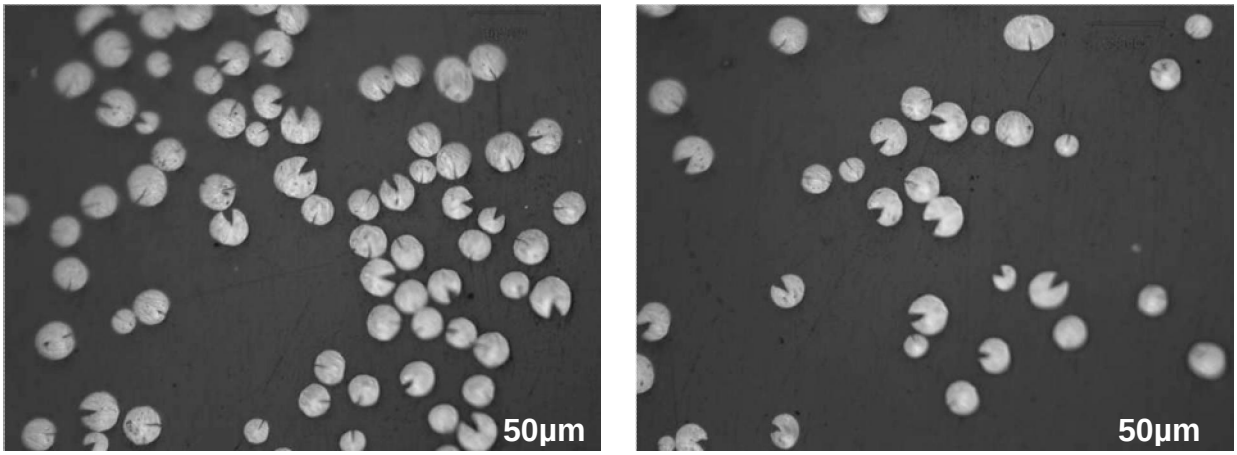

2S2 2S5

Figure 4.3 Typical optical microscope images showing fiber cross-sectional structure

The statistic fiber cross-sectional area for ten prepared carbon fibers is shown in **Figure 4.4**. It can be seen that this Figure is much similar with the **Figure 4.2** (right) which was determined by a laser scan micrometer. The number of fibers representing each method varied from 80-220 fibers thus giving a much larger spread as reflected in the standard deviation. The optical microscope method displays wider distribution (larger deviation) than laser scan micrometer for most carbon fibers measured. This wider variation in fiber cross-sectional area is probably due to the following facts: 1) large number of fibers was examined, and 2) lack of “fiber selective effect”.

In addition, optical microscope method shows smaller average cross-sectional area for most of carbon fibers. The noticeable decrease in cross-sectional area as compared to the laser scan micrometer is in part due to pac-man structures that are not detected with the laser. This differential will be discussed in detail in following sections on the analysis of pac-man structures.

To further validate the optical microscope method, the cross-sectional area of stabilized fiber and its carbonized fibers at different carbonization temperatures were measured. The average and standard deviation are shown in **Figure 4.5.** The histograms of fiber cross-sectional area and calculated fiber diameter distributions are shown in **Figure 4.6**. Cross-sectional area or diameter shrinks as the carbonization temperature increases. It seems that the distribution become narrower as the size of fiber reduced.

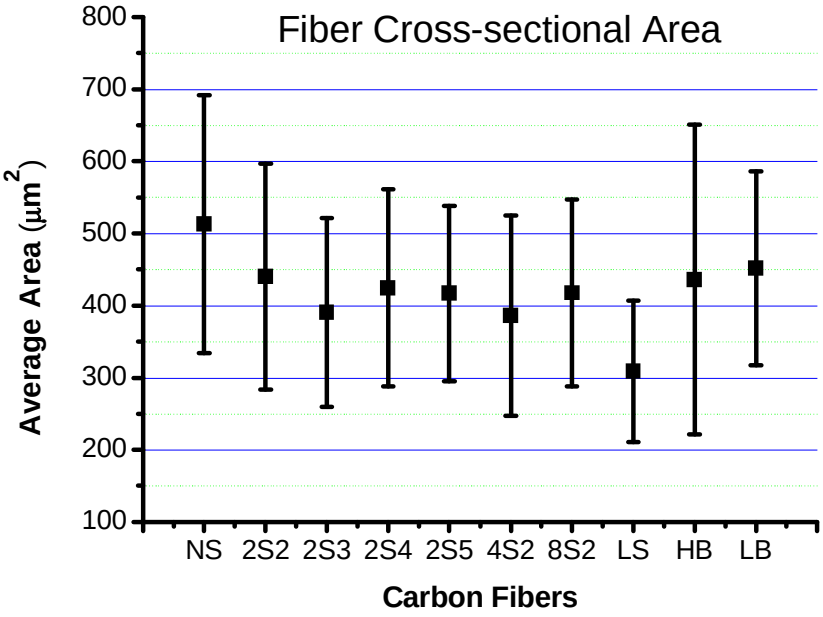

Figure 4.4 Cross-sectional area of carbon fibers (same as in Figure 4.2) measured using optical microscope method

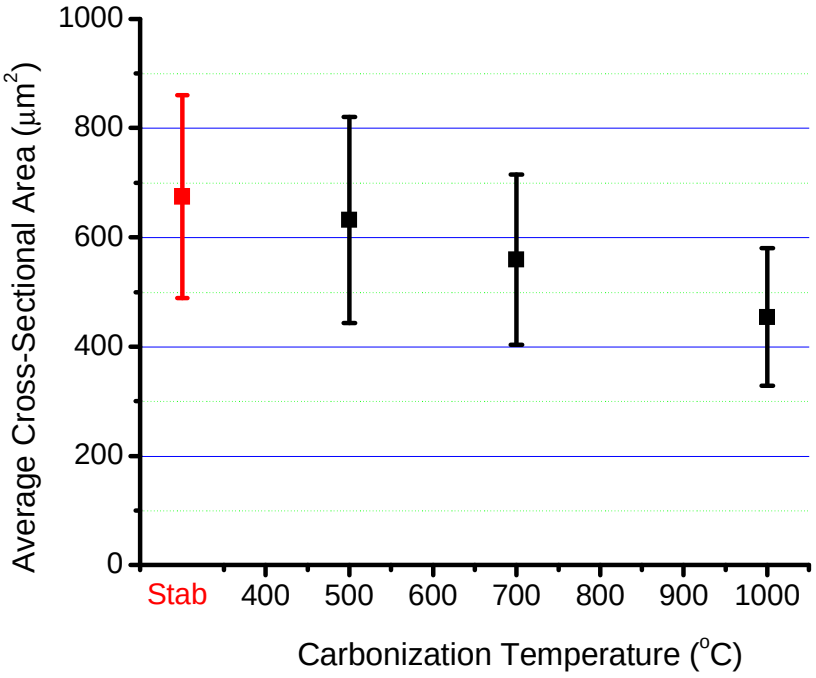

Figure 4.5 Fiber cross-sectional area with deviation measured with optical microscope method vs. carbonization temperatures

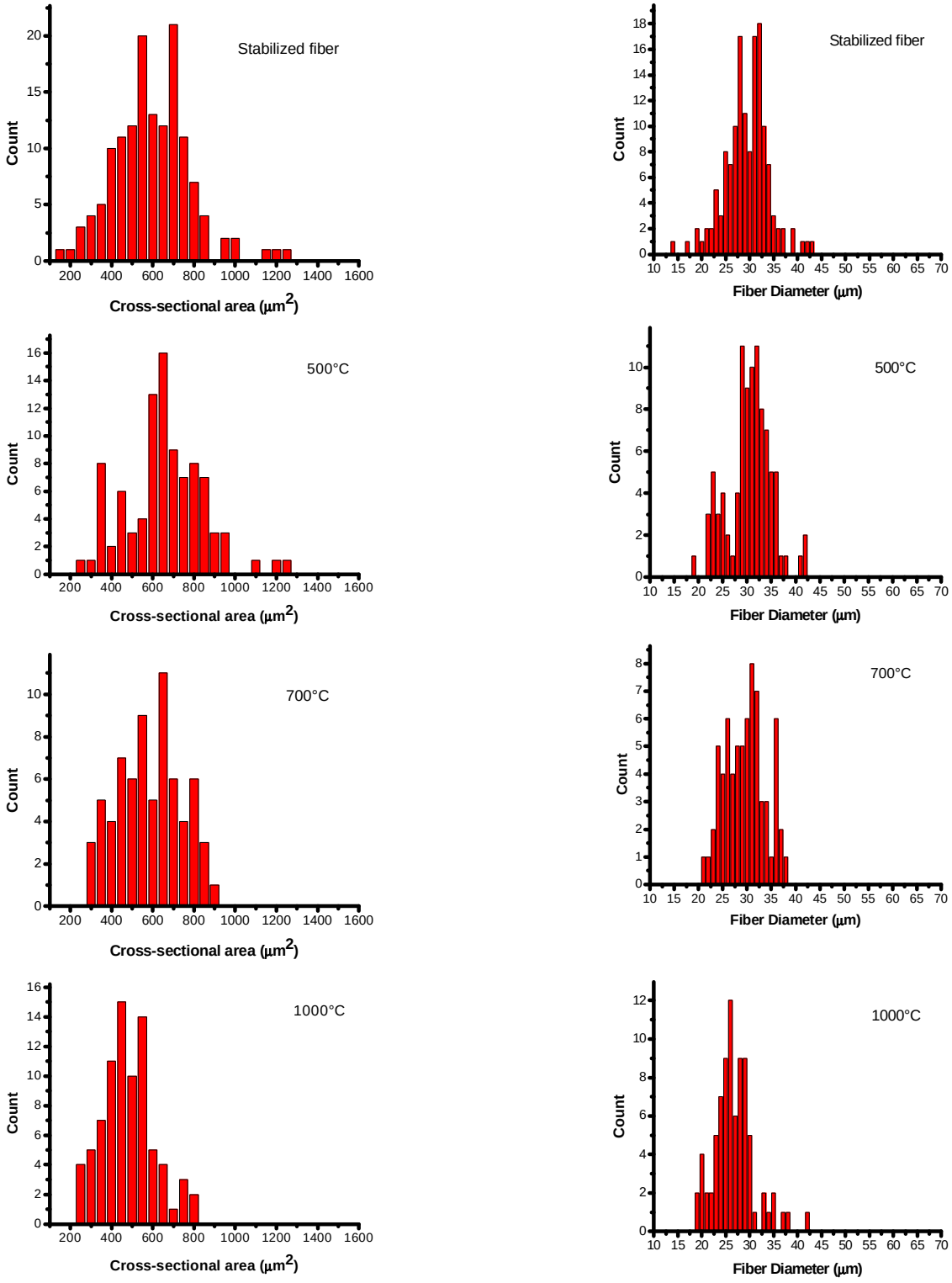

Figure 4.6 Fiber cross-sectional area (left) and diameter (right) distribution histogram changing with carbonization temperatures

4.2 Fiber Diameter Distribution along the Fiber Axis:

Fiber size distribution in a bundle fiber was characterized using a laser scan micrometer and an optical microscope analysis method and discussed in the above section. In the following study, fiber diameter distribution along the fiber axis will be measured in the fiber length of 10 mm with a laser scan micrometer.

4.2.1 Diameter Variation in a Single Fiber:

Samples from UTSI's 40, 60, 80, and 100 LPM carbon fibers were compared against commercial pitch (P-25) and PAN-based carbon fibers with the laser scan micrometer and the results are shown in **Figure 4.7** and **Figure 4.8**. Commercial pitch (P-25) and PAN-based carbon fibers both have a uniform fiber diameter along the fiber length. In contrast, the UTSI carbon fibers lack diameter uniformity along the fiber length. Variations in 40 LPM's fiber diameter are less dramatic from fiber to fiber and along the fiber axis as compared to the other spinning methods. 60 LPM has the biggest spread of fiber diameter along the fiber axis as well as between each fiber sample.

Large diameter variation along the fiber axis could result in nonuniformity of mechanic properties within a single fiber, but it may be of benefit to the fiber composites where bamboo-like fiber acts as anchor (physical bonding) to prevent fiber pulled out from matrix.

4.2.2 3D Plot:

The data obtained from fiber diameter measurement were also used to plot a 3D image (**Figures 4.9 - 4.11**) to well demonstrate the structure of carbon fiber. **Figure 4.9** shows typical 3D ribbon structures of commercial PAN-based and pitch-based carbon fibers. Both fibers look smooth along the fiber axis due to their high diameter uniformity.

However, UTSI carbon fibers show more roughness on the surface due to their lower diameter uniformity along the fiber axis, as shown in **Figure 4.10**. The larger diameter carbon fiber (from 40 LPM) shows relatively smooth surface than other fibers.

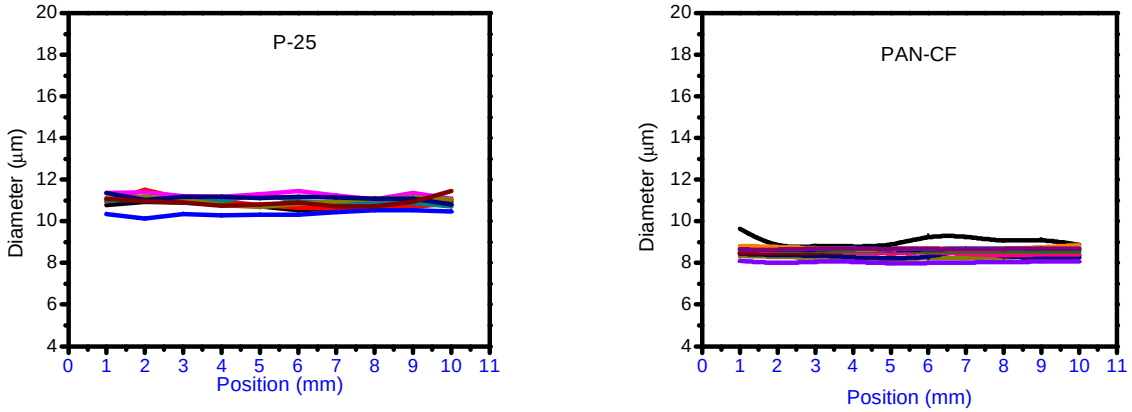

Figure 4.7 Typical graphs showing fiber diameter variation in commercial carbon fibers

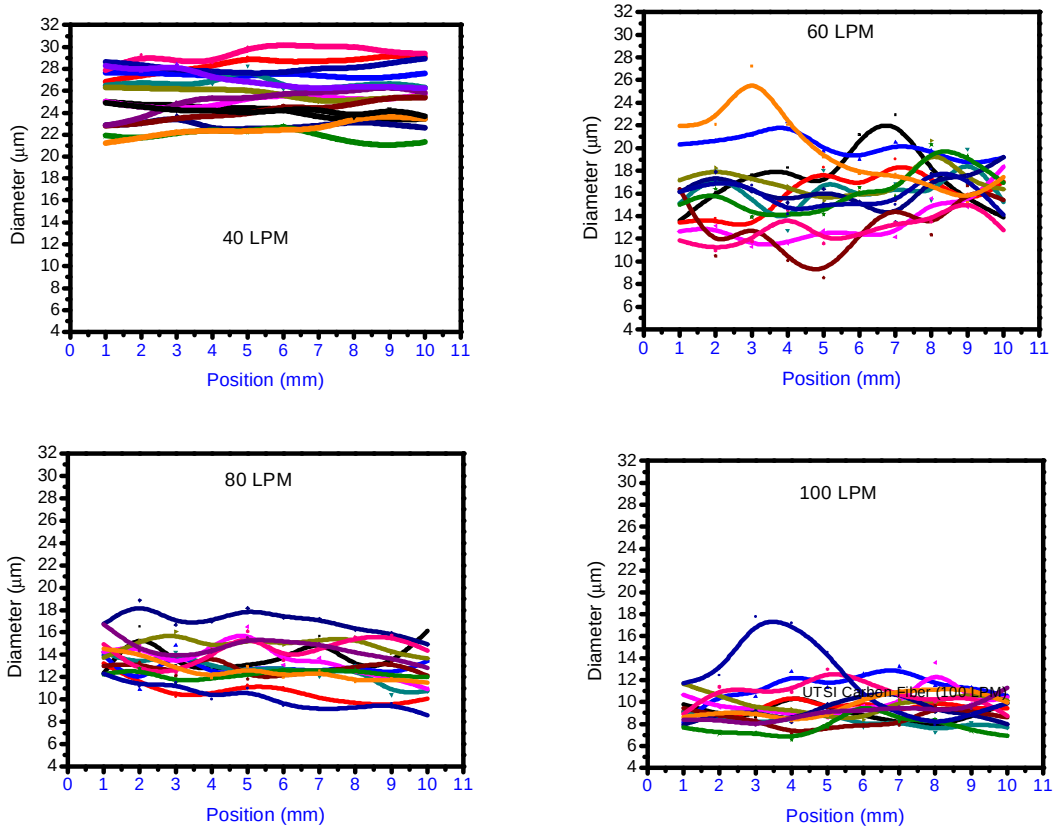

Figure 4.8 Typical graphs showing fiber diameter variation in four UTSI's carbon fibers

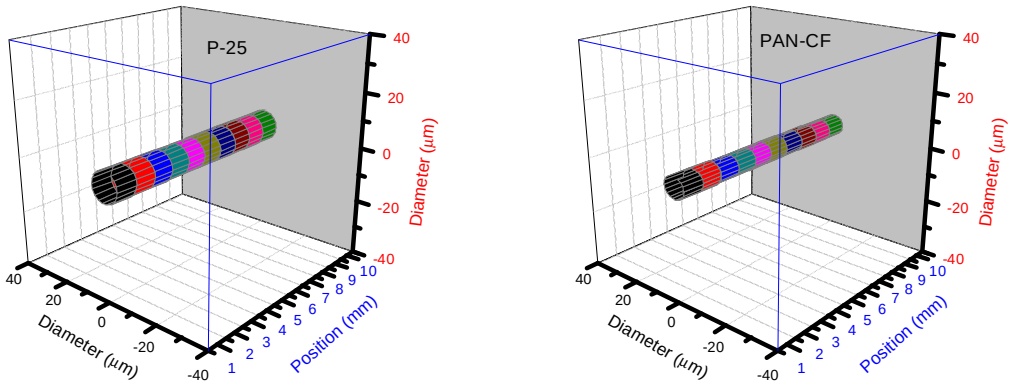

Figure 4.9 Typical ribbon graphs showing 3D structures of commercial carbon fibers

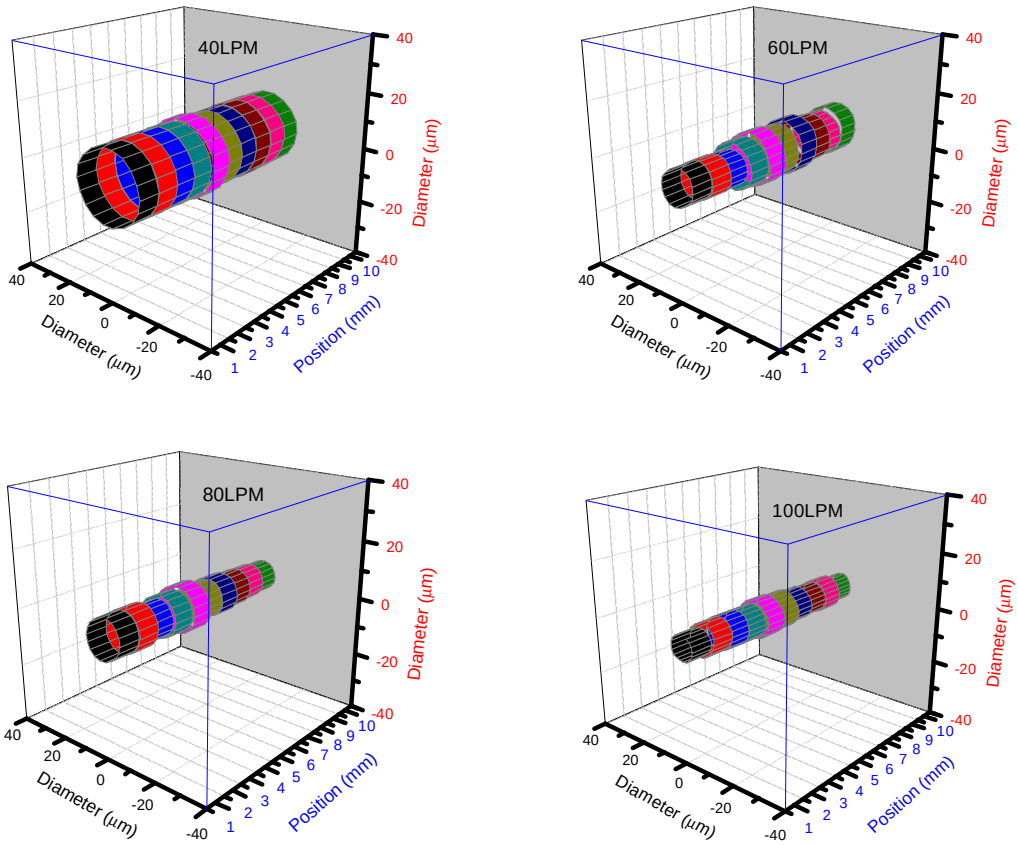

Figure 4.10 Typical ribbon graphs showing 3D structures of four UTSI's carbon fibers

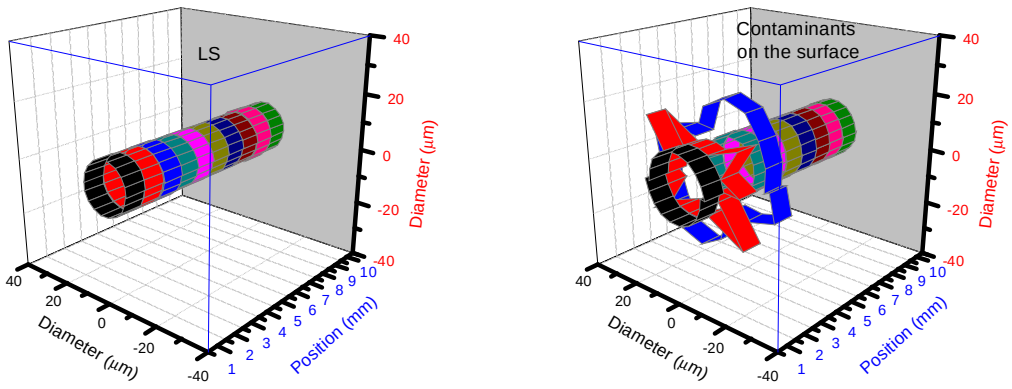

Figure 4.11 Typical ribbon graphs showing 3D structures of special carbon fibers

Additionally, the carbon fiber with long time stabilization (LS) shows smaller diameter and relatively smooth surface (**Figure 4.11**). With this simulation, some specific feature on carbon fiber surface can be demonstrated such as some contaminants shown in **Figure 4.11** (right), which could be dust or wax contamination formed during the preparation for fiber testing.

4.3 Pacman Angle Measurement and Fiber Size Adjustment:

The abundance of pac-man structures seems to have no ill effect on the tensile strength and modulus of the fibers. One reason for this is because the occurrence of the pac-man face is along and not perpendicular to the graphite-like planes of the carbon fibers. However, pac-man structure could reduce the compression strength of carbon fibers which would result in fiber crash during the fabrication of fiber composites with high pressure.

Since the pac-man defects occur along and not across the fiber, the pac-man defect should not negatively impact the calculated tensile strength and modulus of the fiber. On the other hand, error in the laser scan micrometer due to pac-man structures dramatically affects the calculated tensile strength and modulus of fibers.

4.3.1 Theoretical Estimation:

Figure 4.12 illustrates the difference between the laser scan micrometer and the optical microscope. The total surface area of the circle is 3.142*$\mathbf{r}^2$ where **r** is the radius of the circle and average pac-man angle across all methods is approximately 40°. If the fiber cross-section is cut at the red line and the top piece is removed, the surface area of the detached piece is 0.027*$\mathbf{r}^2$, the remaining surface area is 3.115*$\mathbf{r}^2$, and the loss in total surface area is 0.86% which is a negligible amount. Both the laser scan micrometer and the optical microscope can detect the loss in the surface area. With a negligible loss in surface area the error between the two methods also becomes negligible. However, if the entire 40° piece of the circle is removed, as in the case of pac-man structures, then the reduction in surface area is 0.349*$\mathbf{r}^2$, the remaining surface area is 2.793*$\mathbf{r}^2$, and the loss in total surface area is 11.1% which is significantly than the previous case. This difference is readily detected with the optical microscope as pac-man structures are detectable with a software “ImageJ”. This is not the case with the laser scan micrometer because the laser would only scan across the top of the fiber and provides the same estimation as the initial case with the truncated piece.

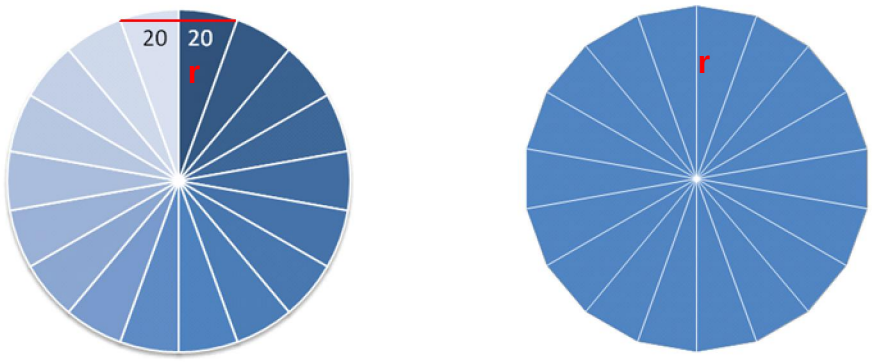

Figure 4.12 Example fiber cross-sectional area with a circular fiber (left) and a octadecagon fiber (right)

The other source of error is the degree of rotation for the fiber. For this experiment the diameter reading was taken at every 20° rotation by the laser scan micrometer. **Figure 4.12** (right) shows an Octadecagon with radius **r**. If the Octadecagon is aligned properly with the laser as shown then the diameter reading would be 2***r** with a surface area of 3.142*$\mathbf{r}^2$. However, if the Octadecagon is rotated by 10° the new diameter reading would be 1.97***r** resulting in a surface area of 3.047* $\mathbf{r}^2$ instead of 3.142*$\mathbf{r}^2$. Fiber alignment and radial defects becomes an issue for all non-circular objects observed with the laser scan micrometer. Since the UTSI carbon fibers exhibit both of these characteristics, the laser scan micrometer is prone to error providing overestimated surface areas for the tensile strength and modulus calculations.

4.3.2 Pacman Angle:

Pac-man angles were measured for seven carbon fibers made using one, two, four, and eight step stabilization methods. The angle average and standard deviation are listed in **Figure 4.13** and compared against the average cross-sectional areas measured with the laser scan micrometer and optical microscope method, respectively.

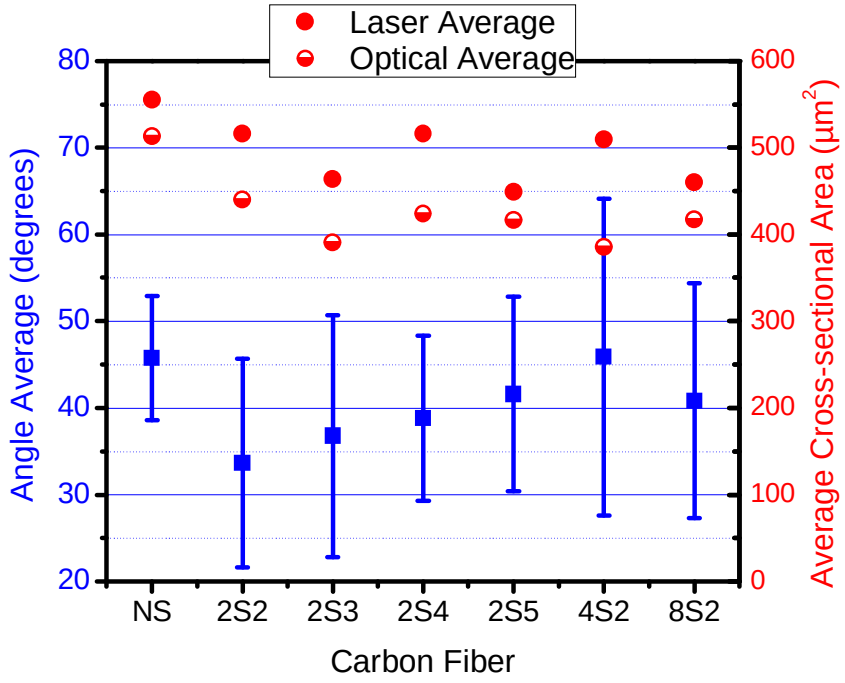

Figure 4.13 Pac-man angle vs. cross-sectional area

For all samples, the laser scan micrometer shows higher average fiber cross-sectional area than the optical microscope method because of the existence of pac-man defect. There is no direct correlation between the angle of the pac-man defect and the resulting cross-sectional areas. For instance, the pac-man angle decreases from NS to 2S2 as the cross-sectional areas also decreases but from 2S2 to 2S3 the pac-man angle increases while the cross-sectional areas continue to decrease.

4.3.3 Cross-sectional Area Adjustment:

Based on the pac-man angle measurement in **Figure 4.13**, laser scan micrometer cross-sectional area can be adjusted to give a more accurate reading of the cross-sectional area as compared to the optical microscope cross-sectional area. This can be done by assuming a circular fiber and then subtracting the area occupied by pac-man structures with the various average pac-man angles. The result of such an adjustment is shown in **Figure 4.14** and the error between the adjusted and regular laser vs. optical is show in **Figure 4.15**.

Using the original laser scan micrometer measurements improvement of 8.36-47.23% can be obtained if the laser scan measurements match that of the optical microscope average. The adjusted laser method provides a 50% error reduction vs. the original laser scan measurements as compared against optical. Improvements of 2.32-17.99% can be obtained if the adjusted laser measurements match the optical microscope average.

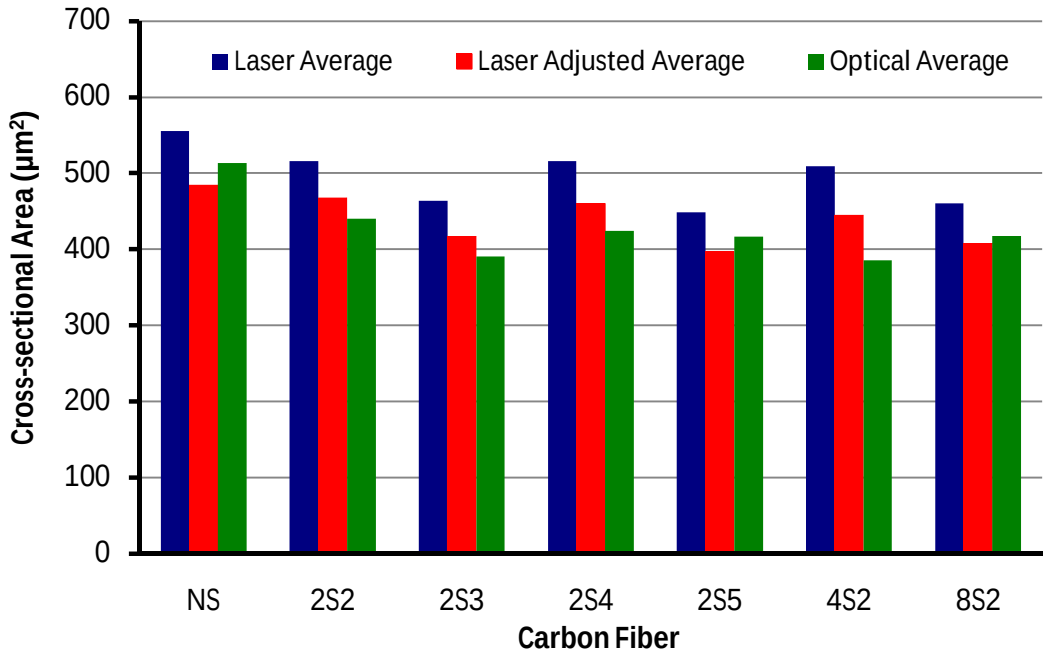

Figure 4.14 Cross-sectional areas of laser, optical, and laser adjusted average

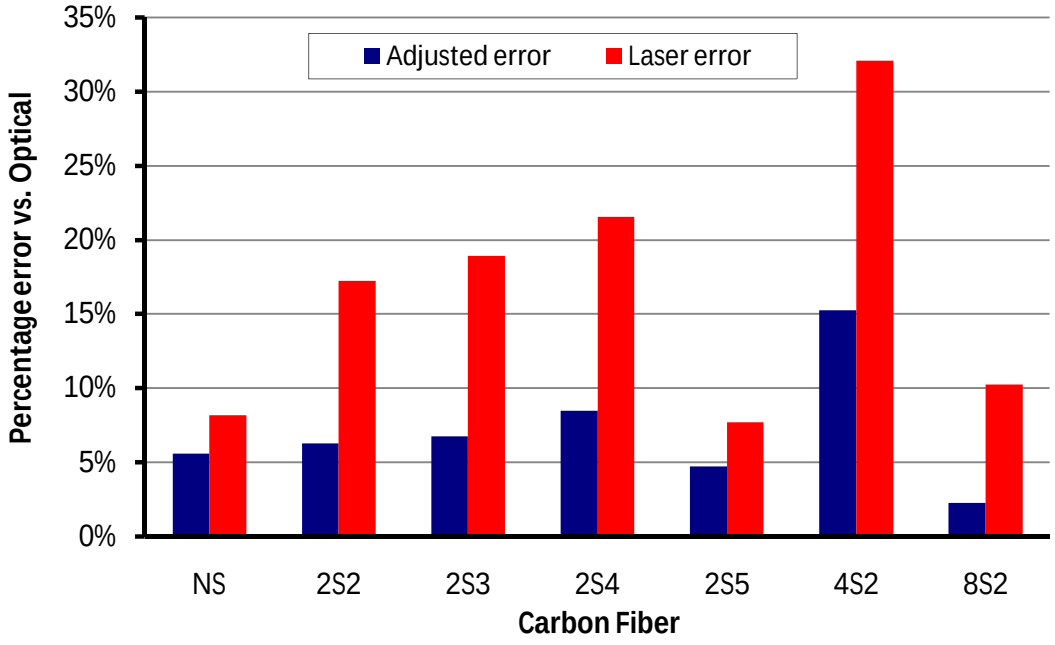

Figure 4.15 Adjusted and laser error

Chapter 5: Preliminary Study on Carbon Fiber Sandwiched Composites (CFSCs)

In the Chapters 3 and 4, the structure and properties characterization of carbon fibers indicates that UTSI carbon fiber exhibits some unusual structural characteristic. How to use this novel carbon fiber is of great interest to our current research. A previous study performed by UTSI carbon fiber research group indicated that the fabrication of UTSI carbon fiber composite with different polymer resins is relatively simple due to its special fiber form. The prepared composites have low density and a high electrical conductivity [17, 22-25]. In this Chapter, a preliminary research on carbon fiber sandwiched composites (CFSCs) was carried out by utilizing the UTSI and commercial PAN-based carbon fibers.

A sandwich structured composite is usually fabricated by attaching two thin and stiff skins to a thick lightweight core. The core material is normally a low strength material but the higher thickness provides the sandwich composite with high bending stiffness while maintaining a low overall density. Sandwich structured composites (SSCs) have been widely used in aerospace structures, ship building, infrastructure, due to their light weight and high strength to weight ratio.

The study on CFSCs is to fabricate sandwich structured composites using UTSI, mesophase pitch-based carbon fiber composites as core materials and single layer of commercially available PAN-based carbon fabric composites as skin materials. The result should be a new sandwich composite that has high bending stiffness, and a low overall density.

5.1. Structure:

UTSI carbon fiber sandwiched composites (CFSCs) have a similar structure with commercial sandwich structured composites but with a solid core as shown in **Table 5.1**. Since the core and skin fibers were fabricated to CFSCs at same time under a high pressure, this process is much simpler than the conventional (multi-step) methods for the sandwich fabrication.

Table 5.1 Structures of the CFSCs and the content of UTSI-CF

CFSC	Content of UTSI-CF (based on the total fiber)	Cross-sectional structure	Thickness of CFSC (mm)
S0	**No core** only two sheets of PAN-CF fabric 0 wt % of UTSI-CF	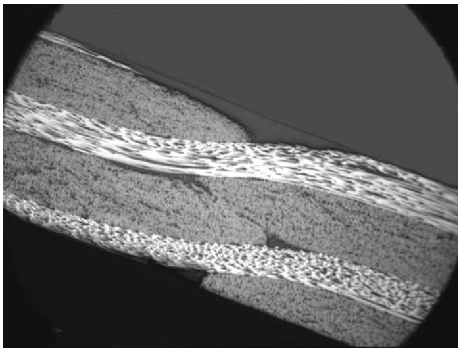	~1.1
S1	Sandwich 20 wt% of UTSI-CF	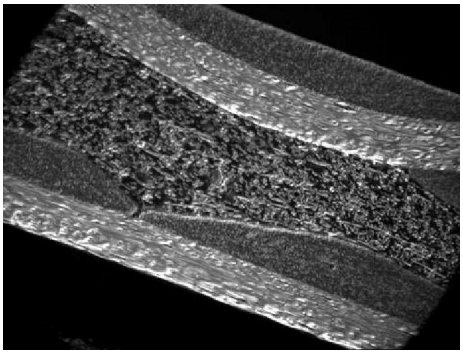	~ 2.1
S2	Sandwich 33 wt% of UTSI-CF	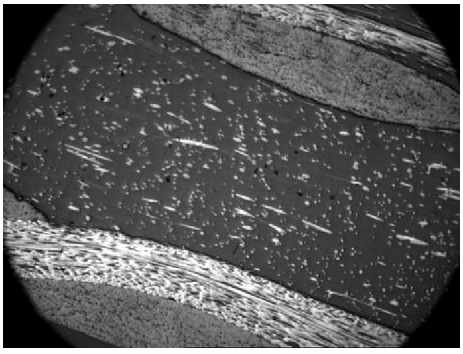	~ 2.8

Table 5.1 shows the ratio of UTSI –CF to the total fiber used, the thickness of the CFSCs, and the composite structures S1 and S2 are CFSCs with PAN-CF fabric skin, UTSI pitch fiber core, and epoxy resin present but S0 is not a CFSC since it was only fabricated by two sheets of PAN-CF fabric and epoxy. The thickness of the composites increased with increasing the amount of the UTSI-CF in the core materials.

For S0 (no core) composite, some structure problem is present and shown in **Figure 5.1**. Epoxy resin domains exists in the interface between the two layers of PAN-CF fabrics. However, this structure defect is not found in the CFSCs S1 and S2.

5.2. Properties:

5.2.1 Flexural and Other Physical Properties:

The physical and flexural properties of the CFSCs are listed in **Table 5.2**. As expected, the apparent density, electrical resistivity, and flexural strength decreased with increasing amount of the core materials, since the core materials, UTSI–CF composites, have lower density, lower resistivity, and lower flexural properties than the PAN-CF skin material. S1 shows the highest value for the flexural modulus. The actual reason is not clear. The removal of structure defects (epoxy domains) may result in the increase in the interlayer shear modulus of the S1.

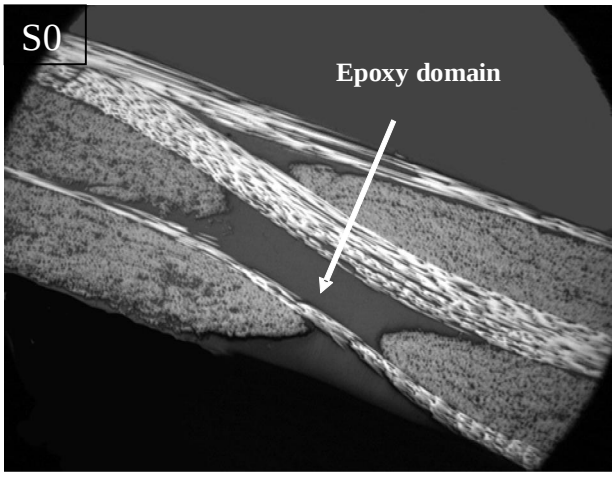

Figure 5.1 Structure problem in S0 (no core) composite

Table 5.2 Physical and flexural properties of the CFSCs

CFSC	Apparent density (g/cm^3)	e-resistivity (Ω*cm)	Flexural strength (MPa)	Flexural modulus (GPa)
S0	1.55	0.06	637	60
S1	1.51	0.05	500	70
S2	1.40	0.03	430	49

5.2.2 Flexural Stiffness:

Two CFSCs (S1 and S2) and one PAN-CF composite (S0) without a core were tested using 3-point bending method with two loading configurations. The typical force-displacement curves recorded in the same support span length are shown in **Figure 5.2**. As expected, the CFSCs with cores exhibit a higher stiffness than PAN-CF composite without a core.

The calculated flexural stiffness, ***D***, the transverse shear rigidity, ***U***, and the core shear modulus, ***G*** based on six samples as specified by ASTM D 7250 are listed in **Table 5.3**. The CFSCs show 10 to 20 time increases in flexural stiffness as compared with PAN-CF composites S0 due to an increase in the thickness of the CFSCs. The CFSCs, S1 and S2, also show higher transverse shear rigidity and the core shear modulus than PAN-CF composite S0.

5.3. Failure of CFSCs:

The failure of CFSCs shown in **Figure 5.3** depends on many factors which includes the core properties and thickness. The failure always appears on the top skin (A) around mid-span due to a compression force during flexural testing with a long support span length. However, when testing in a short support span length, core shear failure (B) was found, and the crack (C) and (D) can propagate through the core layer with increased beam deflection.

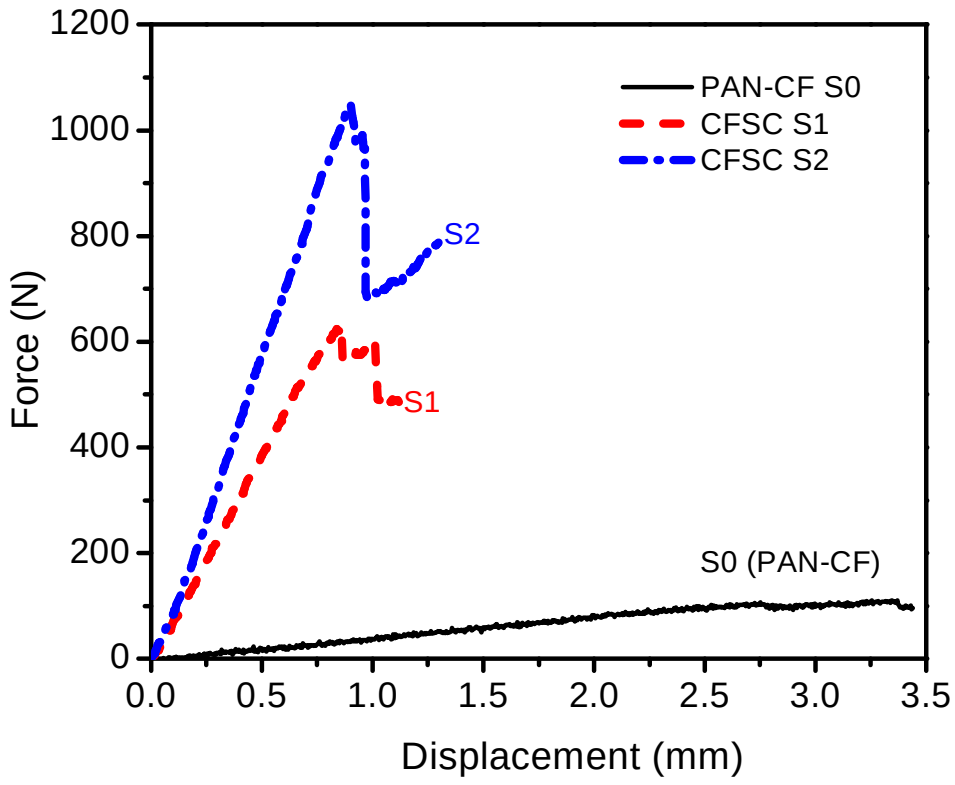

Figure 5.2 Typical force-displacement curves recorded in a same support span length

Table 5.3 Flexural stiffness, transverse shear rigidity, and the core shear modulus of carbon fiber sandwiched composites

Setup	Thick-ness (mm)	Flexural stiffness			Transverse shear rigidity		Core shear modulus	
		N-m^2	StDev	Norma-lized	KN	StDev	Mpa	StDev
S0	1.10	**0.047**	0.006	**1**	9.22	1.05	-	-
S1	2.03	**0.483**	0.056	**10.3**	30.58	12.16	1318	518
S2	2.87	**0.946**	0.167	**20.1**	33.84	15.50	2392	841

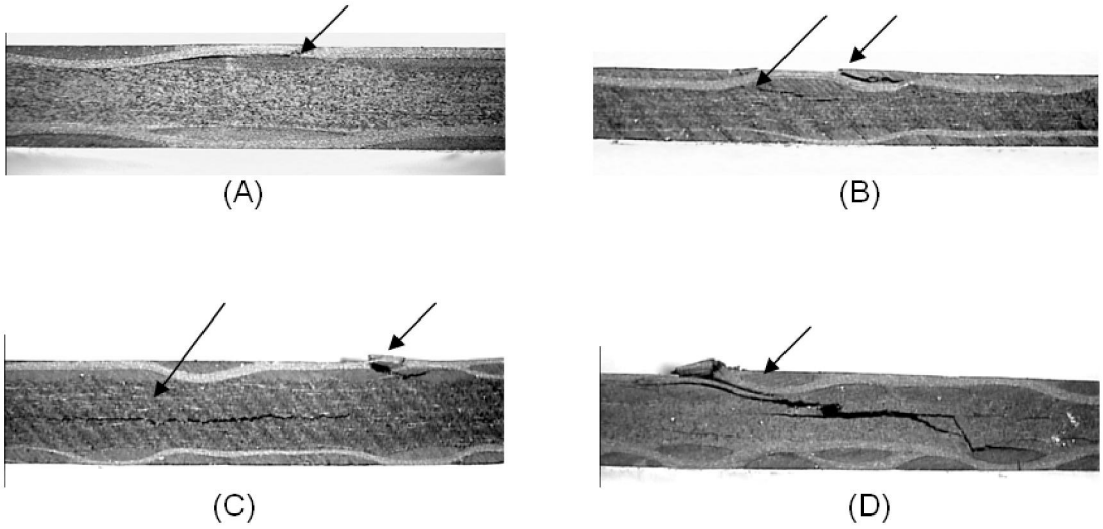

Figure 5.3 Failure of CFSCs showing (A) testing in a long support span length; (B), (C), and (D) testing in a short support span length, with increasing beam deflection

Chapter 6: Conclusion

In this study, pitch-based carbon fiber and its composites were prepared and their structure and properties were characterized using various techniques such as, optical microscope, Dia-stron, SEM, MTS and software ImageJ. Three aspects of research activity were carried out to elucidate the relationship among process, structure, and property in the manufacturing of carbon fiber and its composites. The first and main focus of this work is the effect of thermal process on structure and properties of fibers; the second is the characterization of carbon fiber structure uniformity; and the third is a preliminary work on carbon fiber sandwiched composites.

Carbon fibers were prepared from solvated mesophase pitch fibers (green fibers) through stabilization (dry and oxidation in air) and carbonization (in N_2) processes. The resulting carbon fibers show higher carbon yield of ~ 75 wt % (or ~ 87 wt% if disregarding the solvents). Fiber diameter mainly depends on the melt blowing speeds in the fiber spinning process. It is also affected by the thermal processes and reduces with increasing carbonization temperatures.

Pac-man structure was observed during the carbonization processes. It develops at 600°C and the angle becomes larger as the carbonization temperatures increased. It was found that pac-man structure is easily formed in larger diameter fiber. It is also affected by stabilization conditions. In the case of larger diameter fiber, sheath-core structure are observed in the stabilized fiber due to controlled diffusion of oxidation. Such sheath-core structure can relate with the appearance of pac-man structure of the resulting carbon fibers. Long time, fully stabilized fiber or small diameter fiber doesn't show any sheath-core structure, as a result, no pac-man structure is observed after carbonization.

Hollow carbon fiber was obtained from very short time stabilized fiber. The core without drying and oxidation melts to form a hollow core during the carbonization process.

Mechanical properties of the resulting carbon fibers strongly depended on the stabilization processes including the stabilization methods, temperatures, and duration.

There is a significant improvement from the one to two-step stabilization and then additional improvements were made from two to four-step and four to eight-step stabilization. The multi-step stabilization could give the various reactions that occur during stabilization at different stabilization temperatures sufficient time to react at each temperature range. Stabilization time was a critical factor. The tensile strength and modulus improved as the stabilization duration increased. However, too long stabilization results the decrease in tensile strength due to the over oxidation. Temperature range bias experiments confirmed that giving the lower temperature range more stabilization time resulted in carbon fibers with higher mechanical properties.

Structure uniformity of carbon fibers were determined with two different methods namely, laser scan micrometer and optical microscope. UTSI carbon fiber presents wider distribution in fiber diameter (cross-sectional area) for a bundle fiber or along a single fiber than commercial pitch and PAN-based carbon fibers. Optical microscope method is better than laser scan micrometer to measure and statistically analyze the fiber diameter (cross-sectional area) and its distribution, especially for noncircular fiber or fiber with pac-man structure. 3-D plot obtained from laser scan micrometer data can well demonstrate the fiber diameter and its uniformity.

In the case of large diameter fiber, the existence of pac-man structures in carbon fibers accounts for a significant portion in cross-sectional area. The inability to detect such axial defects by the laser scan micrometer presents a certain degree of error in the estimation of the actual tensile strength and modulus of individual fibers. The actual cross-sectional area was determined with optical microscope and pac-man angle measurement. Statistical analysis reveals that an additional 8.36-47.23% improvement in mechanical properties can be obtained if the cross-sectional area measured with laser scan micrometer be adjusted with a factor.

Carbon fiber sandwiched composites (CFSCs) were fabricated by using UTSI carbon fiber as a core material and commercial PAN-based carbon fiber as skin materials. The fabrication process is simple. The CFSC is of solid core structure. The comprehensive properties were obtained including high flexural strength and modulus, lower density, high electrical conductivity, and a great improvement in flexural stiffness.

References

1. Peter Morgan, Carbon fibers and their Composites, CRC Press, Taylor & Francis Group, LLC, 2005, p269
2. http://inventors.about.com/library/inventors/bllight2.htm
3. John D. Russell, Composites Affordability Initiative: Transitioning Advanced Aerospace Technologies through Cost and Risk Reduction, The AMMTIAC Quarterly, Volume 1, Number 3, 3-6.
4. http://news.thomasnet.com/IMT/archives/2006/10/aircraft_design_king_of_sky_boeing_dreamliner_versus_airbus_a350xwb.html
5. Cohn, S. M. and S. Das, A Cost Assessment of PAN Carbon Fiber Production Technologies: Conventional and Microwave Cases, draft paper, Oak Ridge National Laboratory, Oak Ridge, TN, Feb. 1999.
6. Bunsell, A. R., Fibre Reinforcements for Composite Materials, Amsterdam, The Netherlands: Elsevier Science Publishers B.V., 1988, p. 90.
7. Vakili, A., Low Cost Mesophase Pitch-based Carbon Fiber, TANCON 2006, Knoxville, TN.
8. Fei, Y., Meganathan A. and Vakili, A., Structure of Mesophase Pitch-Based Carbon Fibers Produced via Melt Blow-Spinning, *Carbon Conference*, 2007.
9. Deborah D. L. Chung, Carbon fiber composites, Butterworth-Heinemann, 1994
10. Daniel Gay, Suong V. Hoa, Stephen W. Tsai, Composite materials design and applications, CRC PRESS 2003.
11. Vinson, J.R., Sandwich structures: Past, present, and future, Sandwich Structures 7: Advancing with Sandwich Structures and Materials, 2005, page 3–12. Proceedings of the 7th International Conference on Sandwich Structures, Aalborg University, Aalborg, Denmark, 29-31 August 2005. Edited by O.T. Thomsen et al. Published by Springer 2005
12. Matsumoto, T., and Mochida, I. Oxygen Distribution in Oxidatively Stabilized Mesophase Pitch Fiber. Carbon, Vol.31, No.1, pp.143-147, 1993.

13. Liedtke, V., and Huttinger, K.J. Mesophase Pitches as Matrix Precursor of Carbon Fiber reinforced Carbon: II. Stabilization of Mesophase Pitch Matrix by Oxygen Treatment. Carbon, Vol.35, No.9, pp.1067-1079, 1996.
14. Singer, L.S., and Mitchell, S. Diffusion of Oxygen into Pitch. Carbon, Vol.35, No.5, pp.599-604, 1997.
15. Blanco, C., Lu, S., Appleyard, S.P., and Rand, B. The stabilisation of carbon fibres studied by micro-thermal analysis. Carbon, Vol.42, pp.165-171, 2003.
16. Oak Ridge Workshop Results, Low cost carbon fiber composites for energy applications, March 3-4, 2009.
17. Vakili, A., Yue, Z., Fei, Y., Cochran, H., Allen, L., and Duran, M. Pitch based carbon fiber processing and composites. *SAMPE* 2007, Baltimore, MD, June 3-June 7, 2007.
18. Duran, Matthew P., Production and Optimization of Continuous Roving-like UTSI Pitch-based Carbon Fiber Composites. Masters of Science in Mechanical Engineering, The University of Tennessee, August 2009
19. FTA final report, Low Cost Carbon Fiber Technology Development for Carbon Fiber Composite Applications, *FTA Project Number*: TN-26-7028-2007.1, August 31, 2007
20. Carbon fibers and their Composites, Peter Morgan, 2005, Chapter 4, page 121
21. Yoon, S.H., Korai,Y. and Mochida, I. Assessment and Optimization of the Stabilization Process of Mesophase Pitch Fibers by Thermal Analyses. *Carbon*, Vol.32, No.2, pp. 281-287, 1994.
22. Yue, Z., Duran, M.P., Vakili, A., Fabrication of low-cost composites using roving-like mesophase pitch-based carbon fibers, *ICCE-17 proceedings*, Page 1171, July 26-August 1, 2009. Honolulu, Hawaii, USA
23. Vakili A, Yue Z, and Matthew DP., Influence of fiber surface treatments on low-cost carbon fiber composites, *ICCE-17 proceedings,* Page 1061, 17th

International Conference on Composites or Nano Engineering, July 26-August 1, 2009. Honolulu, Hawaii, USA.

24. Yue, Z, Vakili, A, and Liu, C., Characteristics of Melt-blow Spun Solvated Mesophase Pitch-based carbon Fiber and its Composites, *Carbon 2010 proceedings*, ID 651, The Annual World Conference on Carbon, July 11-16, 2010, Clemson University, SC, USA.

25. Yue, Z, Vakili, A, and Liu, C., Fabrication and Characterization of Lightweight, Cost-effective Carbon Fiber Sandwiched Composites, Accepted by *SAMPE* 2010, Salt Lake City, UT, Oct.11-14, 2010.

Vita

Chang Liu was born in Beijing, China on January 29th of 1986. He received his Bachelor of Science from Georgia Institute of Technology in May of 2008 in Industrial and Systems Engineering. From there he came to University of Tennessee Space Institute in pursuit of a Master of Science in Material Science Engineering on August of 2008.

He is currently planning a long vacation from academia and the decadent economy after obtaining the Masters of Science to travel the world in pursuit of things other than knowledge and money.